

1                   **HYDROCHEMICAL BEHAVIOUR OF LONG-LIVED NATURAL**  
2                   **RADIONUCLIDES IN SPANISH GROUNDWATERS**

3  
4           S.M Pérez-Moreno<sup>1</sup>, J.L Guerrero<sup>1</sup>, F. Mosqueda<sup>1</sup>, M.J. Gázquez<sup>2</sup> y J.P. Bolívar<sup>1</sup>

5                   <sup>1</sup>Departament of Integrated Sciences, University of Huelva, Huelva, Spain.

6                   <sup>2</sup>Department of Applied Physics, University of Cadiz, University Marine Research  
7   Institute (INMAR) Cádiz. Spain.

8  
9  
10   **ABSTRACT**

11   This research was focused on the analyses the hydrochemical behaviour of long-lived  
12   natural radionuclides (<sup>210</sup>Po, <sup>210</sup>Pb, <sup>234,238</sup>U, <sup>230,232</sup>Th, <sup>226,228</sup>Ra) in groundwaters located in  
13   Spanish aquifers with different geological characteristics and evaluate the dose by  
14   ingestion of these waters. The study was performed by the gross alpha-beta, alpha  
15   spectrometry and physicochemical analysis of a set of bottled drinking waters.  
16   Radionuclide activities in the investigated aquifers were highly variable. High  
17   concentration of <sup>210</sup>Pb is associated with granitic bedrock and reducing conditions. On  
18   the other hand, the highest <sup>238,234</sup>U concentrations were found in carbonate aquifers.  
19   Activities of <sup>226</sup>Ra are largely controlled by ion exchange reactions due to the presence  
20   of relatively high concentration of chloride. Several waters exceeded the parametric value  
21   for gross alpha mainly due to <sup>234</sup>U, <sup>226</sup>Ra and/or <sup>210</sup>Pb concentrations. Moreover, the  
22   content of <sup>226</sup>Ra and <sup>210</sup>Pb in the water contributed mainly to the indicative dose.

23   **KEYWORDS:** *Groundwater, Natural Radioactivity, long-lived radionuclides, Alpha*  
24   *spectrometry, Indicative Dose, Spain.*

## 26 1. INTRODUCTION

27 Most European countries as well as in the rest of the world, the consumption of  
28 commercial mineral water from groundwater has increased significantly in the last two  
29 decades. Up to date, more than 2000 natural mineral waters have been recognised in the  
30 EU, where about 52 billion litres were consumed in 2017, corresponding to 26.2 % of the  
31 world's consumption (EFBW, 2019).

32 The mineral composition and properties of each natural mineral water are derived from  
33 the geological conditions present in the area where the water is extracted. The presence  
34 of natural radionuclides in the host rock and their interaction with water allow part of the  
35 natural radionuclides to be transferred into the water (Chau et al., 2011; Rozmaric et al.,  
36 2012). This fact can pose a risk to human health due to the ingestion of water, which is  
37 one of the pathways of incorporation of radioactive substances into the human body (Jia  
38 et al., 2009; Manu et al., 2014). Studying the concentration of natural radionuclides in  
39 drinking bottled water can be used to determine the behaviour of these radionuclides  
40 under different hydrogeological conditions (pH, ionic strength, redox potential, etc.).

41 The effective dose received through this pathway (consumption of bottled groundwater)  
42 is mainly due to  $^{40}\text{K}$ , and both  $^{238}\text{U}$ - and  $^{232}\text{Th}$ -series radionuclides present in drinking  
43 water. Polonium-210 is one of the most radiotoxic natural radioactive isotopes known due  
44 to its relatively long half-life (138 days). Polonium and lead can be distributed throughout  
45 the soft tissue of the body and accumulate in the liver, kidneys and bones. The  
46 accumulation of  $^{210}\text{Pb}$  in the skeleton provides another source of  $^{210}\text{Po}$  over time  
47 (Carvalho et al., 2017). In addition, Ra is also one of the most toxic radioelements due to  
48 its tendency to be accumulated in the bones, since its chemical and biological behaviour  
49 is similar to that of alkaline earth metals (Ca, Sr, Ba) (Altikulac et al., 2015; Stackelberg

50 et al., 2018). Uranium seems to follow the same tendency (IAEA, 2014), as it is retained  
51 in the body primarily in the skeleton (vertebrae, ribs and femur). In addition to these,  
52 thorium is deposited mainly on bone surfaces, where it is retained for long time periods  
53 (Bhatti et al., 2012).

54 In accordance with the Council Directive 2013/51/EURATOM, the contribution to the  
55 exposure of the general public as a whole from practices which involve a risk from  
56 ionising radiation must be kept as low as reasonably achievable. The strategies to indicate  
57 radioactivity levels in drinking water may include screening for certain radionuclides, or  
58 gross alpha-beta activity screening. Gross alpha and beta activities are very useful  
59 parameters for the preliminary screening of waters. From the radiological point of view,  
60 the most significant natural radionuclides in waters are  $^{226}\text{Ra}$ , an alpha emitter ( $t_{1/2} = 1600$   
61 y), and  $^{228}\text{Ra}$ , a beta emitter ( $t_{1/2} = 5.75$  y) (IAEA, 2014). Other radionuclides, such as  
62  $^{210}\text{Pb}$ , a beta emitter ( $t_{1/2} = 22.3$  y), and  $^{210}\text{Po}$ , an alpha emitter ( $t_{1/2} = 138.4$  days), can also  
63 limit the quality of drinking water (Ansoborlo et al., 2012).

64 The EU recommended screening levels for gross alpha activity of  $0.1 \text{ Bq L}^{-1}$  and for gross  
65 beta activity of  $1.0 \text{ Bq L}^{-1}$  in order to keep that the Indicative Dose (ID) lower than  $0.1$   
66 mSv (EURATOM, 2013). However, the concentrations of certain radionuclides, such as  
67  $^{226,228}\text{Ra}$ ,  $^{210}\text{Pb}$  and  $^{210}\text{Po}$ , among others, must be measured through accurate dose  
68 assessments. Recently, Spanish regulations incorporated this directive about  
69 requirements for the protection of the health of the general public with regard to  
70 radioactive substances in water intended for human consumption (RD 314/2016).

71 Studies for measuring the natural radioactivity and estimating the effective dose of bottled  
72 mineral drinking waters have been carried out worldwide (Kozłowska et al., 2007;  
73 Karamanis et al., 2007; Wallner et al., 2008; Vasile et al., 2016). However, those

74 performed in Spain (Baeza et al., 1995; Ortega et al., 1996; Herranz et al., 1997; Dueñas  
75 et al., 1997; Manjón et al., 1997; Martín Sanchez et al., 1999; Palomo et al., 2007), were  
76 all published before the new regulations and the majority were focused on measuring  
77 gross alpha and beta activity.

78 Moreover, the existence of high activity concentration of natural radionuclides in bottled  
79 mineral drinking waters depends on the characteristics of the aquifer and the rock  
80 substrate. The literature consulted (Chau et al., 2011; UNSCEAR, 2016) shows that the  
81 concentration of uranium in igneous rocks is higher than in sedimentary rocks, and felsic  
82 igneous rocks contain significantly more uranium than mafic rocks. Under oxidizing  
83 conditions, insoluble U(IV) species dissolve, giving rise to highly soluble uranyl ion,  
84  $\text{UO}_2^{2+}$ . At pH range between 6 and 8, typical values for groundwater, uranyl ions tend to  
85 form soluble complexes with inorganic ligands (i.e., phosphates and carbonates)  
86 (Markich, 2002; Sherif and Sturchio, 2018). However, in solutions with low ionic  
87 strength, the concentration of U can be limited by cation exchange and adsorption  
88 processes.

89 The concentration of Ra isotopes in groundwater is typically correlated with the  
90 concentration of uranium and thorium isotopes and their decay products in the bedrock.  
91 Ra in dissolution can be produced by alpha recoil of its parent nuclide ( $^{230}\text{Th}$ ), contained  
92 in the solid materials surface of the aquifer since its parent is very insoluble, or can also  
93 reach the solution phase by its direct dissolution from the bedrock (Vinson et al., 2013).  
94 Meanwhile, the presence of radium isotopes in groundwaters depends mainly on the both  
95  $^{230}\text{Th}$  and  $^{226}\text{Ra}$  activity concentrations in the host rock and physicochemical properties  
96 of the aquifer groundwater. The presence of both Fe and Mn hydroxides high  
97 concentrations in the aquifer water tends to reduce the Ra solubility, but, on the other  
98 hand, high ionic strength tends to increase the desorption of Ra-isotopes from the bedrock

99 into the groundwaters (Sturchio et al., 2001; Szabo et al., 2012, Sherif et al., 2019;  
100 Stackelberg et al., 2018). Radium is also controlled by coprecipitation/dissolution  
101 processes. For example, the very low solubility of the barite ( $\text{BaSO}_4$ ), limits the Ra  
102 concentration in the water due to the co-precipitation of Ra bound to barite (Grundl and  
103 Cape, 2006; Grandia et al., 2008, Sherif and Sturchio 2018).

104 In view of these facts, knowledge of the distribution of long-lived natural radionuclides  
105 in groundwater as a function of the geochemical and hydrological Spanish regional  
106 conditions, can help to assess the exposure and to inform to population about the risk of  
107 having waters with high activity concentration of a certain natural radionuclides. So, the  
108 aim of this paper was to evaluate the radiological quality of a significant set of drinking  
109 bottled waters of different Spanish brands with different geological origin, as well as to  
110 study the behaviour of natural radionuclides ( $^{210}\text{Po}$ ,  $^{210}\text{Pb}$ ,  $^{234,238}\text{U}$ ,  $^{230,232}\text{Th}$ ,  $^{226,228}\text{Ra}$ ) of  
111 the groundwater.

## 112 **2. MATERIALS AND METHODS**

### 113 **2.1. SAMPLES**

114 Fifteen different brands of bottled drinking water from different Spanish locations were  
115 purchased in local supermarkets in the area of Huelva in July 2016. Several samples were  
116 taken for each brand to evaluate possible differences in the water properties between  
117 batches. All mineral waters were preserved in their original bottles and their natural state  
118 until the beginning of this work in September 2018. The waters selected are included in  
119 Table 1, as well as the code of each batch and their origin.

120 Figure 1 shows the main lithologies of Spain and the location of the springs where the  
121 bottled drinking waters were taken. As can be observed, the analysed waters belong to  
122 different geologic origin, including igneous (granites), metamorphic (schists), carbonated

123 (limestones and dolomites) and sedimentary (conglomerate and gravels). More details of  
124 the geology of the aquifers can be seen in Figure S1 of Supplementary Information.

125

126 *Table 1. Summarised information of the different brands of bottled water analysed.*

127

128 *Figure 1. General lithological map of Spain and the location of the bottled water sources*  
129 *analysed.*

130

## 131 **2.2. PHYSICOCHEMICAL PARAMETERS**

132 The pH and electrical conductivity (EC) of the bottled water samples were measured  
133 using a previously calibrated CRISON multi parameter electrode, model MM40+. The  
134 trace elements were analysed using an ICP-MS, model Perkin Elmer Sciex ELAN 9000,  
135 from Activation Laboratories Ltd. (Actlab, Canada). Concentrations of anions ( $F^-$ ,  $Cl^-$ ,  
136  $NO_2^-$ ,  $NO_3^-$  and  $SO_4^{2-}$ ) were analysed at the University of Huelva through high-  
137 performance liquid chromatography (HPLC) using a Metrohm 883 basic ion  
138 chromatograph equipped with Metrosep columns. In all measurement techniques several  
139 reference materials were used in order to assure the quality of the results.

140 A piper diagram was performed with EASY QUIM software (GHS, 2019). The Piper  
141 diagram is used as visualisation tool for find out the hydro-chemical of groundwater  
142 samples. The Piper diagram consists of two composition ternary diagrams, along with a  
143 rhombus plot in the middle. The composition ternary on the left is mapped based on  
144 normalised mass fractions of three cationic components ( $Ca^{2+}$ ,  $Mg^{2+}$ ,  $Na^+ + K^+$ ), whilst  
145 the aspect ternary on the right is based on three anionic components ( $Cl^-$ ,  $SO_4^{2-}$ ,  $CO_3^{2-} +$   
146  $HCO_3^-$ ) (Piper, 1953).

147 **2.3. GROSS ALPHA-BETA ACTIVITY**

148 Both the gross alpha and gross beta activities were measured to identify the most active  
149 samples, using a multi-detector low background  $\alpha/\beta$  counting system (Berthold LB770).  
150 The sample detectors were window gas-flow counters with approximately 5.0 cm in  
151 diameter. The counting gas was a mixture of 90% argon and 10% methane. All samples  
152 were placed in a 5 cm diameter stainless steel planchet for counting. The operating voltage  
153 on the detector was selected to be 1700 V.

154 The system was calibrated for simultaneous  $\alpha$  and  $\beta$  measurements by preparing standard  
155 samples with known concentrations of both  $^{241}\text{Am}$  ( $27.5 \pm 0.2 \text{ Bq g}^{-1}$ ) and  $^{90}\text{Sr}/^{90}\text{Y}$  ( $160.8$   
156  $\pm 0.4 \text{ Bq g}^{-1}$ ) solutions. The counting efficiencies were 5–15% for  $\alpha$  and 30–39% for  $\beta$   
157 depending on mass thickness ( $\text{mg}/\text{cm}^2$ ). The background of the detectors presented values  
158 of around 0.02 and 0.2 cpm for  $\alpha$  and  $\beta$  windows, respectively.

159 To determine gross alpha and beta activities, aliquots of each sample were taken, ranging  
160 between 0.2 and 3 L, depending on their dry residue, to achieve a mass thickness of about  
161 6-8  $\text{mg}/\text{cm}^2$ . Then, the samples were evaporated at a controlled temperature up to few  
162 millilitres on a hot plate and then transferred to a striated stainless steel planchet. This  
163 was evaporated to dryness under an infrared lamp. The samples were kept in a desiccator  
164 for a few days, (between 2 and 7 days, in order to avoid the appearance of  $^{222}\text{Rn}$  and its  
165 descendants) and then they were weighed and counted. Alpha/beta counting was  
166 determined by averaging the results obtained from two cycles of 600 min.

167 The determination of the gross alpha/beta activities was conducted following the ISO  
168 norms (UNE EN ISO 10704, 2016; UNE 73340-2, 2003). The validation of the method  
169 was carried out using several samples from intercomparison exercises organised by the  
170 Spanish Nuclear Safety Commission (Consejo de Seguridad Nuclear, CSN) (Table 2).

171 Since no certified water samples were available, the samples consisted of calcareous soil  
172 (CSN-2016), an atmospheric filter (CSN-2017) and milk powder (CSN-2018).

173 **Table 2.** *Gross alpha and beta activity concentrations obtained in the intercomparison*  
174 *exercises organised by the Spanish Nuclear Safety Commission (CSN).*

## 175 **2.4. RADIONUCLIDE CONCENTRATIONS BY ALPHA-PARTICLE**

### 176 **SPECTROMETRY**

177 The radiochemical procedure to isolate both U- and Th-isotopes was based on the  
178 tributylphosphate (TBP) back-extraction methodology (Holm and Fukai, 1977). In this  
179 method, the sample is dissolved in 8M HNO<sub>3</sub>, and then the actinides are extracted into  
180 tributylphosphate (TBP), whereas the aqueous nitric fraction contains the rest of the non-  
181 actinide radioelements (Po, Ra, etc.). Th is back-extracted by using 1.5 M HCl + Xilen,  
182 and then U is back-extracted from the organic phase with distilled water. On the other  
183 hand, Po and Ra remain in the 8M HNO<sub>3</sub> phase, and Po is self-deposited onto silver disks  
184 in 2M HCl by the method proposed by Flynn (1968). The Po remaining in dissolution  
185 contains the Ra-isotopes, which are isolated by cation exchange chromatography, using  
186 resins such as AG50X12 (Pérez-Moreno, 2019). The thin radioactive source for U and Th  
187 was obtained by electrodeposition following the methodology described by Talvitie  
188 (1972) and Hallstadius (1984), whereas the one for Ra was obtained by BaSO<sub>4</sub>  
189 microprecipitation (Blanco et al., 2002). Then, the activity concentrations of the different  
190 isotopes were measured using passivated implanted planar silicon (PIPS) detectors, (EG  
191 & G Ortec). For these determinations, the samples were spiked with accurately known  
192 activities of <sup>232</sup>U ( $138.9 \pm 0.6$  mBq mL<sup>-1</sup>), <sup>229</sup>Th ( $177.6 \pm 1.1$  mBq mL<sup>-1</sup>) and <sup>209</sup>Po ( $105.6$   
193  $\pm 0.7$  mBq mL<sup>-1</sup>).



194 The quality control of the measurements was carried out by using: a) one blank and one  
195 replicate every five samples, b) several samples from the intercomparison exercise  
196 organised by the Spanish Nuclear Safety Commission (CSN) and c) certified reference  
197 materials: phosphogypsum (CSN-2008) and soils (IAEA-326 and IAEA-327) (Table 3).

198 **Table 3.** *Results obtained in the intercomparison exercise and certified reference*  
199 *materials.*

200 The activity concentration of  $^{210}\text{Pb}$  in all water samples was considered to be in secular  
201 equilibrium with  $^{210}\text{Po}$  between the sampling time and the measuring time (2 years). Thus,  
202 the activity concentration of  $^{210}\text{Pb}$  was determined by measuring that of  $^{210}\text{Po}$ .

## 203 **2.5. STATISTICAL ANALYSIS**

204 A principal component analysis (PCA) using XLSTAT was conducted to analyse the  
205 groundwater data. This statistical analysis was carried out to find out if the samples are  
206 related to each other. PCA is a method for reduce a large number of variables, finding  
207 new variables (principal components), which are ordered so that the first few retain most  
208 of the variation present in all of the original variables, making the data easier to  
209 understand (Jolliffe, 2002). The PCA is used to study the relationship between variables  
210 and identify how groups of variables change with respect to each other The Spearman  
211 correlation matrix has been used since the majority of the variables do not follow a normal  
212 distribution (Davis, 2002).

213

## 214 **2.6. INDICATIVE DOSE**

215 According to Directive EURATOM (2013), when the following formula is satisfied  
216 (Concentration Index (CI)) (Eq. 1), it may be assumed that the ID is below the parametric  
217 value of 0.1 mSv and no further investigation shall be required:

$$CI = \sum_{i=1}^n \frac{Ci (obs)}{Ci (der)} \leq 1 \quad \text{Eq. 1}$$

218

219 Where:

220  $C_i (obs)$  = observed concentration of radionuclide  $i$

221  $C_i (der)$  = derived concentration of radionuclide  $i$

222  $n$  = number of radionuclides detected.

223 The CI was calculated for all the water samples analysed. In those cases, in which the  
 224 parametric value was exceeded, the ID was determined according to the measured  
 225 radionuclide concentrations and the dose coefficients established in Annex 3 of RD  
 226 783/2001 (ICRP, 2007), using the following equation, based on 730 L of annual ingestion  
 227 for adults:

$$ID = \sum_j h(g)_j J_j \quad \text{Eq. 2}$$

228

229 Where:

230  $h(g)_j$  = effective dose committed per unit of incorporation by radionuclide  $j$  ( $\text{Sv Bq}^{-1}$ )

231 ingested by an individual belonging to the age group  $g$ ;

232  $J_j$  = the corresponding incorporation by ingestion of radionuclide  $j$  (Bq).

### 233 3. RESULTS AND DISCUSSION

#### 234 3.1. PHYSICOCHEMICAL PARAMETERS

235 The physicochemical parameters and element concentrations for all water samples are  
 236 shown in Figures 2-4, and Table S1 of Supplementary Information, in which the waters

237 were classified according the lithology. The pH ranged from 6.5 to 7.5, showing the  
238 neutral character of the studied waters. The waters from carbonate aquifers shows an  
239 average slightly higher ( $7.2 \pm 0.1$ ) (uncertainty expressed as the standard deviation of the  
240 mean) than waters from granite aquifers ( $6.7 \pm 0.2$ ). The electrical conductivity (EC) of  
241 the samples ranged from 19 to  $289 \mu\text{S cm}^{-1}$ , with an average of  $84 \pm 20 \mu\text{S cm}^{-1}$  for waters  
242 from granite bedrock and  $231 \pm 24 \mu\text{S cm}^{-1}$  for carbonate bedrock. The dry residue (DR)  
243 varied from 35 to  $724 \text{ mg L}^{-1}$  (average =  $179 \pm 43 \text{ mg L}^{-1}$  in granite aquifers and  $507 \pm$   
244  $62 \text{ mg L}^{-1}$  in carbonate aquifers). Waters from carbonate bedrock present highest values  
245 of these parameters in relation to waters from granite aquifers. Concretely, CAZ, VEL  
246 and SIS waters presented the highest pH (pH = 7.2 -7.4), EC ( $274\text{-}289 \mu\text{S cm}^{-1}$ ) and DR  
247 ( $591\text{-}724 \text{ mg L}^{-1}$ ), whereas AQA and SIF showed the lowest values for these three  
248 parameters (pH = 5.8-6.6; EC =  $19\text{-}25 \mu\text{S cm}^{-1}$ ; DR=  $35\text{-}54 \text{ mg L}^{-1}$ ). This can be observed  
249 in Figure 2, where higher pH shows higher EC and DR and vice versa.

250 **Figure 2.** *pH, EC and DR values of the bottled waters analysed.*

251 The relationship between pH, EC and DR mainly depend on the presence of ions in the  
252 solution. The concentrations of the major elements and ions are shown as box and whisker  
253 plots (Figure 3). The top and bottom of the box are the first quartile (Q1) and the third  
254 quartile (Q3), respectively, and the distance between them is the Interquartile Range  
255 (IQR). Data beyond the  $1.5 \cdot \text{IQR}$  may be considered as outliers (extreme values),  
256 extending the whiskers to the highest and lowest values. The existence of high maximum  
257 values for concentrations of these elements in some waters causes mean values to be much  
258 higher than the median. According to the median values, the elements and ions can be  
259 ordered from highest to lowest concentrations as follows:  $\text{HCO}_3^- > \text{Ca} > \text{SO}_4^{2-} > \text{Cl} > \text{Mg}$   
260  $> \text{NO}_3^- > \text{Na} > \text{Si} > \text{K} > \text{F}$ . The Shapiro-Wilk normality test results (Table S2-

261 Supplementary Information) indicated that, with the exception of  $\text{NO}_3^-$  and  $\text{HCO}_3^-$ , these  
262 ions do not follow a normal distribution.

263 In most cases, the high concentration of bicarbonate and calcium ions are relevant with  
264 respect to the other ions. The bicarbonate concentration ranged from  $13 \text{ mg L}^{-1}$  to  $409 \text{ mg}$   
265  $\text{L}^{-1}$ , while calcium concentration varies from  $1.0 \pm 0.2 \text{ mg L}^{-1}$  to  $88 \pm 4 \text{ mg L}^{-1}$ . The highest  
266 concentration of these ions is found in waters from carbonated aquifers ( $\text{HCO}_3^-$ :  $284 \pm 39$   
267  $\text{mg L}^{-1}$ ; Ca:  $69 \pm 8 \text{ mg L}^{-1}$ ) (NAT, SOL, CAZ, AQB, VEL, SIS). In addition, the  
268 concentration of magnesium is especially high in these waters ( $15 - 46 \text{ mg L}^{-1}$ ). The high  
269 mean concentration of  $\text{HCO}_3^-$  ( $195 \pm 33 \text{ mg L}^{-1}$ ), Ca ( $41 \pm 9 \text{ mg L}^{-1}$ ) and Mg ( $27 \pm 5 \text{ mg}$   
270  $\text{L}^{-1}$ ) is clearly related to the dissolution of the carbonated (limestone and dolomite) host  
271 rocks of aquifers. These relations can be clearly observed in the correlation matrix of  
272 principal component analysis (PCA) and Figures S1 and S2 of Supplementary  
273 Information. This fact is associated with the dominant presence of  $\text{HCO}_3^-$  in the pH range  
274 of water intended for human consumption (pH = 6-8).

275 On the other hand, Na and Cl, which are typically related to the dissolution of evaporites  
276 and salts, showed low correlation in the waters studied (Figure S3a- Supplementary  
277 Information). Na and Cl showed a minimum value (average:  $3.9 \pm 0.9 \text{ mg/L}$  and  $7.7 \pm 2.4$   
278  $\text{mg/L}$ , respectively) in aquifers from carbonate bedrock and maximum (average:  $24 \pm 8$   
279  $\text{mg/L}$  and  $9.8 \pm 1.8$ , respectively) from granite aquifers.

280 The  $\text{SO}_4^{2-}$  ion is usually associated in aquifers with the dissolution of sulphate evaporites  
281 (mainly gypsum) interbedded with carbonated host rocks. The  $\text{SO}_4^{2-}$  concentration  
282 showed a mean concentration of  $3.7 \pm 1.3 \text{ mg L}^{-1}$  in waters from granite aquifers, and  $28$   
283  $\pm 6 \text{ mg L}^{-1}$  in waters from carbonate bedrock. In the studied waters, good correlations of

284  $\text{SO}_4^{2-}$  ion with Ca were found (Figure S3b- Supplementary Information), indicating the  
285 dissolution of calcium sulphates compounds in the studied waters.

286 In contrast, Si showed clearly higher concentrations in the waters from igneous and  
287 metamorphic host rocks, with a maximum of  $30 \pm 2 \text{ mg L}^{-1}$  (AGS). In addition, Si shows  
288 certain correlations with Na and K (PCA matrix correlation), suggesting the dissolution  
289 of silicates.

290 **Figure 3.** *Box and whisker plots of major elements and ions.*

291 Figure 4 shows the Piper diagrams. In the anionic diagram it can be seen that most of the  
292 analysed waters were carbonated; only two were chlorinated, and one was mixed. On the  
293 other hand, calcium was the most abundant cation, according to the cationic diagram,  
294 whereas some waters contained high concentrations of sodium and potassium cations.  
295 Thus, from the central diagram, 57.1 % of the waters were classified as calcium  
296 bicarbonated (AQB, CAZ, REG, NAT, VEL, LAN, SIS and SOL), 21.4 % as sodium  
297 bicarbonated (AGS, CAB and MON), 14.3 % as calcium chlorinated (AQA and VIR) and  
298 7.1 % as sodium chlorinated (SIF).

299 **Figure 4.** *Piper diagram of the bottled water sources.*

300 Waters from SIF displayed a relatively high concentrations of Al, As and Mn ( $143 \mu\text{g L}^{-1}$ ,  
301  $2.9 \mu\text{g L}^{-1}$  and  $14.5 \mu\text{g L}^{-1}$ , respectively). Even though SIF has the highest As  
302 concentration among the investigated aquifers, the As level is still below maximum  
303 contaminant level of As in drinking water (Table S1-Supplementary Information). The  
304 presence of As is probably due to conditions that favour the desorption or dissolution of  
305 Al and Mn oxides and/or oxyhydroxides, in which As is adsorbed (Bowell et al., 2014).  
306 The occurrence of strongly reducing conditions at near-neutral pH leads to the desorption

307 of As from mineral oxides (Smedley and Kinniburgh, 2002). Presumably, similar  
308 conditions caused Pb to be released into the aquifer where AQA was taken (Clausen et  
309 al., 2011). In addition, it is worth highlighting the presence of Li and Cs in AGS, CAB  
310 and MON, which are waters characterized by high concentrations of Na in solution (Fig.  
311 4). In those cases, Li and Cs seem to have the same behaviour as sodium (PCA matrix  
312 correlation), which is probably related to the dissolution of silicates in which they are  
313 bonded (Deverel et al., 1990). The content of Ba in LAN, REG, VEL and MON, Sr in  
314 NAT, and Ni in VEL is mainly determined by the dissolution of  $\text{BaCO}_3$ ,  $\text{SrCO}_3$  and  
315  $\text{NiCO}_3$  from the host rock, respectively. Several studies have confirmed that the presence  
316 of bicarbonate ions in groundwaters ensures the existence of  $\text{Ba}^{2+}$ ,  $\text{Sr}^{2+}$  and  $\text{Ni}^{2+}$  in  
317 solution, forming highly soluble salts (Man and Hooda, 2010; Giménez-Forcada and  
318 Vega-Alegre., 2015; Tudorache et al., (2018)).

319 On the other hand, the concentrations of Cd, Cr, Cu, Fe, Hg and Se were below the  
320 detection limit (0.01; 0.5; 0.2; 10; 0.2; 0.2  $\mu\text{g L}^{-1}$ , respectively).

321 In general, the salinity range indicates that the investigated waters are below the  
322 parametric value established in RD 1798/2010 (de 30 de diciembre). Thus, all the bottled  
323 waters analysed in this work are considered potable from the physicochemical point of  
324 view.

### 325 **3.2. GROSS ALPHA-BETA ACTIVITY CONCENTRATION**

326 Gross alpha and gross beta activity concentrations in the water samples are shown in  
327 Figure 5 and Table S3 of Supplementary Information. The gross alpha activity  
328 concentration ranged from  $10 \pm 2 \text{ mBq L}^{-1}$  (VIR) to  $195 \pm 13 \text{ mBq L}^{-1}$  (VEL) with an  
329 average of  $69 \pm 22 \text{ mBq L}^{-1}$  and  $80 \pm 21 \text{ mBq L}^{-1}$  for granite and carbonate aquifers  
330 respectively, although in three water samples (AGS, BEZ and SIS) it was below the

331 detection limit ( $DL = 10 \text{ mBq L}^{-1}$ ). Three of the investigated aquifers (MON, SIF, and  
332 VEL) exceeded the EU recommended level for gross alpha ( $0.1 \text{ Bq L}^{-1}$ ). The high level  
333 of alpha activity is likely related to the lithologic composition and hydrogeological  
334 parameters of the bedrock (Chau et al., 2011). In these cases, the geology is governed by  
335 carbonated rocks (limestone and dolomite) located in the centre of Spain and igneous  
336 rocks (granite) located in the west, north and centre (Baeza et al., 1995; Dueñas et. al,  
337 1997).

338 On the other hand, the gross beta activity concentration of the water samples ranged from  
339  $41 \pm 1 \text{ mBq L}^{-1}$  (VIR) to  $585 \pm 10 \text{ mBq L}^{-1}$  (VEL), with an average of  $157 \pm 43 \text{ mBq L}^{-1}$   
340 in waters from granite bedrock and  $191 \pm 63 \text{ mBq L}^{-1}$  in the carbonate bedrock. In contrast  
341 with the gross alpha activity, the gross beta activity concentration of all investigated  
342 samples is below the EU recommended value for drinking water of  $1 \text{ Bq L}^{-1}$ . It is worth  
343 highlighting that those waters with higher gross beta activity also had higher K and Na  
344 concentrations. The gross beta activity is very related to K concentration since the  $^{40}\text{K}/\text{K}$   
345 isotopic ratio in nature is constant, i.e.  $320 \text{ Bq/kg}$  of  $^{40}\text{K} = 1\%$  of natural K. This fact,  
346 joined to the concentration of the radionuclide  $^{40}\text{K}$  is generally 1-2 orders of magnitude  
347 higher than the remaining natural beta-emitters, justify the good fitting found between  
348 gross beta and  $^{40}\text{K}$  concentration,  $\text{Gross beta} = (0.78 \pm 0.10) [^{40}\text{K}] + (-10 \pm 33)$  ( $R^2 =$   
349  $0.90$ ). Na is really related to K since both elements belong to the silicate compound  
350 present in the bedrock, giving this fact an indirect correlation with the gross beta, formed  
351 mainly by the contribution of  $^{40}\text{K}$ .

352 **Figure 5.** Gross  $\alpha$  and  $\beta$  activity concentrations of the analysed water samples ( $DL= 10$   
353  $\text{mBq L}^{-1}$ ).

354 These results are consistent with those of previous works (Andreo and Carrasco, 1999;  
355 Martín Sanchez et al., 1999; Palomo et al., 2007), where the gross alpha and beta activities  
356 of some mineral waters were analysed (AGS, AQA, BEZ, CAB, LAN, MON, SOL and  
357 VEL), and which confirm that higher alpha activity concentrations generally correspond  
358 to areas where granitic formations are predominant. This is due to the fact that granitic  
359 rock is characterized by a high concentration of radionuclides of the  $^{238}\text{U}$  series (Korkmaz  
360 Gorur et al., 2011; Sherif and Sturchio, 2018).

361

### 362 3.3. RADIONUCLIDE ACTIVITY CONCENTRATIONS

363 The concentrations of natural radionuclides ( $^{210}\text{Pb}$ ,  $^{234,238}\text{U}$ ,  $^{230,232}\text{Th}$ ,  $^{226,228}\text{Ra}$ ) in the  
364 bottled waters were measured by alpha-particle spectrometry and are shown in Table 4  
365 and Figure 6.

366 **Table 4.** Activity concentrations ( $\text{mBq L}^{-1}$ ) of  $^{210}\text{Pb}$ ,  $^{238-234}\text{U}$ ,  $^{228-226}\text{Ra}$ , activity ratios of  
367  $^{234}\text{U}/^{238}\text{U}$ ,  $^{226}\text{Ra}/^{234}\text{U}$ ,  $^{210}\text{Pb}/^{226}\text{Ra}$  and  $^{226}\text{Ra}/^{228}\text{Ra}$  ( $DL = 1 \text{ mBq L}^{-1}$ ) and Concentration  
368 Index (CI). \*Derived Concentrations (DC) for radioactivity in water intended for human  
369 consumption (RD 314/2016).

370 The activity concentrations of  $^{210}\text{Pb}$  ranged from  $1.4 \pm 0.5$  (BEZ) to  $78 \pm 3 \text{ mBq L}^{-1}$  (SIF),  
371 with an average value of  $20 \pm 7 \text{ mBq L}^{-1}$  (uncertainty expressed as the standard deviation  
372 of the mean) in waters from granite bedrock and  $5.6 \pm 0.7 \text{ mBq L}^{-1}$  in carbonate aquifers.  
373 The activity concentration of 52 % of the bottled waters analysed was below  $10 \text{ mBq L}^{-1}$   
374 and that of 33 % was below the detection limit ( $1 \text{ mBq L}^{-1}$ ). The lowest activities of  $^{210}\text{Pb}$   
375 were measured in waters, where sedimentary rocks exist, whereas the highest activities  
376 were measured in aquifers of granitic bedrock, especially the ones located in Extremadura  
377 (AQA and SIF). This zone consists mainly of acidic plutonic rock (basically granite),



378 formations of low-grade metamorphism, and tertiary and quaternary sedimentary  
379 materials, notably alluvia, limestone, clay and materials from the erosion of shale and  
380 granite with a range of  $^{238}\text{U}$  activity concentration of 60-80 Bq kg<sup>-1</sup> (Baeza et al., 1995;  
381 CSN, 2000; Galán López and Martín Sánchez., 2008). Therefore, high values of  $^{210}\text{Pb}$  in  
382 these waters are attributed to the high rates of supply due to higher total U concentrations  
383 in solids, and possibly high desorption rates of  $^{210}\text{Pb}$  (Porcelli, 2014). In this sense, AQA  
384 and SIF present high Mn concentration, indicating possibly reducing conditions in which  
385  $^{210}\text{Pb}$  is released.

386 The activity concentrations of  $^{238}\text{U}$  ranged from  $1.8 \pm 0.2$  (AQA) to  $33 \pm 2$  mBq L<sup>-1</sup>  
387 (REG), with an average of  $7.5 \pm 3.3$  mBq L<sup>-1</sup> (granite aquifers) and  $9.9 \pm 1.8$  mBq L<sup>-1</sup>  
388 (carbonate aquifers), whereas those of  $^{234}\text{U}$  ranged between  $1.8 \pm 0.3$  (BEZ) and  $55 \pm 4$   
389 mBq L<sup>-1</sup> (SOL), with an average of  $11 \pm 5$  mBq L<sup>-1</sup> (granite aquifers) and  $22 \pm 6$  mBq L<sup>-1</sup>  
390 (carbonate aquifers). Furthermore, the concentration of three waters (CAB, VIR and  
391 AGS) was below the detection limit (1 mBq L<sup>-1</sup>). It is worth highlighting the values of  
392  $^{238}\text{U}$  and  $^{234}\text{U}$  in REG water, with a concentration of  $33 \pm 2$  mBq L<sup>-1</sup> and  $53 \pm 3$  mBq L<sup>-1</sup>  
393 respectively; and in SOL water, whose concentrations for  $^{238}\text{U}$  and  $^{234}\text{U}$  were  $20 \pm 2$   
394 mBq L<sup>-1</sup> and  $55 \pm 4$  mBq L<sup>-1</sup>. The activity concentration of  $^{238}\text{U}$  was in agreement with  
395 the uranium concentration measured by ICP-MS ( $R = 0.95$ ), with an intercept value of -  
396  $0.38 \pm 1.1$  and a slope of  $15 \pm 1$ . These data are in line with the conversion factor of  
397 radioelement concentration given by IAEA (2003).

398 Some samples displayed a clear disequilibrium between  $^{238}\text{U}$  and  $^{234}\text{U}$ . The  $^{234}\text{U}/^{238}\text{U}$   
399 activity ratio ranged from  $0.95 \pm 0.22$  to  $3.1 \pm 1.3$  (Table 4); in most cases it was greater  
400 than unity. The disequilibrium between these two isotopes in water is due to the  
401 preferential leaching of  $^{234}\text{U}$ , favored by alpha recoil effects (Chau et al., 2011,

402 UNSCEAR, 2016). The highest activity concentrations of  $^{234}\text{U}$  were found in waters from  
403 springs formed in carbonated rock, where the greatest disequilibrium between  $^{238}\text{U}$  and  
404  $^{234}\text{U}$  was found (SOL, CAZ, AQB, VEL and SIS). The high activity concentration of U  
405 isotopes in waters from carbonated aquifers may be attributed to the formation of soluble  
406 carbonate complexes such as  $\text{UO}_2(\text{CO}_3)_2^{2-}$  and  $\text{UO}_2(\text{CO}_3)_3^{4-}$  under oxidising conditions  
407 and neutral pH (Shabana and Kinsara, 2014; Guerrero et al., 2016; Wu et al., 2018; Eröss  
408 et al., 2018).

409 In some waters, the secular equilibrium between  $^{238}\text{U}$  and  $^{234}\text{U}$  is reached, specifically  
410 NAT, LAN, BEZ, SIF and MON. This may occur as a result of two factors: 1) the long  
411 residence time of the water in the aquifer, greater than the half-life of  $\text{U}^{234}$ , and 2) low  
412 concentration of  $\text{U}^{238}$  in the aquifer solids, thus both isotopes could reach the equilibrium  
413 in the dissolved phase.

414

415 The activity concentrations of Th-isotopes ( $^{228}\text{Th}$ ,  $^{230}\text{Th}$  and  $^{232}\text{Th}$ ) were below the  
416 detection limit ( $1 \text{ mBq L}^{-1}$ ) in all waters. This is due to the fact that Th has only one stable  
417 oxidation state (IV) under all redox conditions in natural waters. Therefore it has a very  
418 low mobility under most environmental conditions, mainly due to the high stability of the  
419 insoluble oxide  $\text{ThO}_2$  (Santschi et al., 2006; Bhatti et al., 2012).

420 The activity concentrations of  $^{226}\text{Ra}$  ranged from  $1.1 \pm 0.1 \text{ mBq L}^{-1}$  (VIR) to  $194 \pm 9 \text{ mBq}$   
421  $\text{L}^{-1}$  (MON) (average of granite aquifers:  $35 \pm 17 \text{ mBq L}^{-1}$ ; average of carbonate aquifers:  
422  $20 \pm 9 \text{ mBq L}^{-1}$ ). The activity concentration of 56 % of the analysed waters was lower than  
423  $10 \text{ mBq L}^{-1}$  and that of only 7.4 % of the samples was below the detection limit ( $1 \text{ mBq}$   
424  $\text{L}^{-1}$ ). The occurrence of Ra in groundwater depends on the concentration of the parent in  
425 the rock matrix, but also on variations in Ra supply to water by alpha recoil,  
426 adsorption/desorption, ion exchange and dissolution/precipitation processes (Sherif et al.,

427 2018). The relation of Ra concentrations with dominant solutes present in the waters can  
428 reflect the hydrochemical factors that control their presence (Sherif and Sturchio, 2018).  
429 The highest activity concentration was found in waters with granitic rock interaction,  
430 specifically in the northeast of Spain (AQA, SIF and MON). This fact is expected since  
431 the highest concentrations of  $^{238}\text{U}$  (progenitor of  $^{226}\text{Ra}$ ) are found in these kinds of rocks,  
432 concretely about  $60\text{-}80\text{ Bq kg}^{-1}$  of  $^{238}\text{U}$  in Extremadura and  $80\text{-}350\text{ Bq kg}^{-1}$  of  $^{238}\text{U}$  in  
433 Galicia (Stackelberg et al., 2018; CSN, 2000; Taboada et al., 2006). However, VEL,  
434 which interacted with carbonate rock, also presented a high activity concentration of  
435  $^{226}\text{Ra}$ , possibly due to the preferential leaching of  $^{234}\text{U}$ . But also, the cation exchange  
436 process could be affecting the presence of radium since there is a high correlation of  $^{226}\text{Ra}$   
437 with  $\text{Cl}^-$  concentration (Figure S2 – Supplementary Information).

438 The activity concentration of  $^{228}\text{Ra}$  varied between  $1.2 \pm 0.5\text{ mBq L}^{-1}$  (CAB) and  $52 \pm 4$   
439  $\text{mBq L}^{-1}$  (MON) (Table 4), with an average of  $17 \pm 5\text{ mBq L}^{-1}$  in waters from granite  
440 bedrock and  $6.7 \pm 1.6\text{ mBq L}^{-1}$  in the carbonate bedrock one. The activity concentration  
441 of 70 % of the waters was below  $10\text{ mBq L}^{-1}$ , 26 % was between  $10\text{-}50\text{ mBq L}^{-1}$ , and 4%  
442 was above  $50\text{ mBq L}^{-1}$ . As in the case of  $^{226}\text{Ra}$ , the highest concentrations of  $^{228}\text{Ra}$  were  
443 found in waters from granite bedrock (AQA, REG and MON) and exceptionally in a  
444 carbonate aquifers (VEL), probably because of the existence of high ion strength that  
445 tends to increase the desorption of Ra isotopes (Vinson et al., 2013). These waters from  
446 carbonate aquifers presented the lowest  $^{228}\text{Ra}/^{226}\text{Ra}$  activity ratio ( $\ll 1$ ) (Table 4). This  
447 fact is related to the preferential leaching of  $^{226}\text{Ra}$  from the host rock with respect to  $^{228}\text{Ra}$   
448 in waters with high carbonate concentrations, but also depend on the both  $^{228}\text{Ra}$  and  $^{226}\text{Ra}$   
449 half-lives (5.7 y, and 1600 y, respectively). (Chau et al., 2011; Sherif et al., 2018).  
450 However in most granite aquifers, the  $^{226}\text{Ra}/^{228}\text{Ra}$  isotopic ratio was close to one. This

451 fact is related to the ratio of the activity concentrations of its parent  $^{232}\text{Th}/^{238}\text{U}$  in the  
452 bedrock, and it is typically close to the unity for granitic or siliceous materials.

453 Most of the waters with granitic host rock presented a high disequilibrium between  $^{226}\text{Ra}$   
454 and  $^{234}\text{U}$  (AQA, MON and SIF) (Table 4), which indicates the preferential leaching of  
455 radium over uranium. However, NAT presented an activity concentration of  $^{226}\text{Ra}$  in  
456 secular equilibrium with the decay series parents ( $^{238}\text{U}$  and  $^{234}\text{U}$ ), since they have equal  
457 activities ( $^{234}\text{U}/^{238}\text{U} \sim 1$ ;  $^{238}\text{U}/^{226}\text{Ra} \sim 1$ ), which means that the aquifer is sufficiently old  
458 ( $>10^5$  years) to reach the secular equilibrium between all the radionuclides of the  $^{238}\text{U}$   
459 series.

460 Furthermore, some waters from aquifers located in Extremadura (e.g., AQA and SIF)  
461 with high concentrations of  $^{226}\text{Ra}$  also showed high concentrations of  $^{210}\text{Pb}$ , although  
462 these did not seem to be in equilibrium (Table 4). The conditions of these aquifers suggest  
463 that the redox conditions are slightly predominant by comparison with the ion strength  
464 in which  $^{210}\text{Pb}$  and  $^{226}\text{Ra}$  are released into the water respectively.

465 The existence of high maximum values for concentrations of  $^{210}\text{Pb}$ ,  $^{226}\text{Ra}$  and  $^{228}\text{Ra}$  causes  
466 mean values to be far above the median (Figure 6), which indicates that the distribution  
467 is very asymmetric. According to the Shapiro-Wilk normality test results (Table S2,  
468 Supplementary Information) none of these natural radionuclides follow a normal  
469 distribution.

470 **Figure 6.** *Box and whisker plots of natural radionuclide activity concentrations.*

471 Waters with high concentrations of  $^{226}\text{Ra}$ ,  $^{234}\text{U}$  and/or  $^{210}\text{Po}$  (MON, SIF, and VEL)  
472 indicated gross alpha in excess of the recommended level. In addition, the gross alpha  
473 calculated ( $G\alpha_{\text{calculated}}$ ) from the activity concentration of alpha emitter radionuclides

474 contained in the waters presented a strong correlation with the gross alpha measured  
475 ( $G\alpha_{\text{calculated}} = (1.6 \pm 19) + (0.92 \pm 0.21) \cdot G\alpha_{\text{measured}}$ ;  $R^2 = 0.65$ ).

476 The natural radionuclides activity concentrations found in the bottled waters analysed  
477 were similar to those ones measured in previous studies in the Spanish region (Ortega et.  
478 al., 1996; Manjon et al., 1997) and other studied aquifers (Khandaker et al., 2017; Jankovic  
479 et al., 2012; UNSCEAR, 2008; Jia and Torri 2007; Kralik et al., 2003; Somlai et al.,  
480 2002), not being in any case above the EU maximum level ( $^{238}\text{U}$  activity  $3.0 \text{ Bq L}^{-1}$ ,  $^{234}\text{U}$   
481 activity  $2.8 \text{ Bq L}^{-1}$ ,  $^{226}\text{Ra}$  activity  $0.5 \text{ Bq L}^{-1}$ ,  $^{228}\text{Ra}$  activity  $0.2 \text{ Bq L}^{-1}$ ,  $^{210}\text{Pb}$  activity  $0.2$   
482  $\text{Bq L}^{-1}$ ,  $^{210}\text{Po}$   $0.1 \text{ Bq L}^{-1}$ ) given by a dose of  $0.1 \text{ mSv}$  (EURATOM, 2013).

### 483 3.4. STATISTICAL ANALYSIS

484 A principal component analysis (PCA) was carried out to summarize the relationships  
485 between the measurement variables (Jolliffe, 2002), in order to detect relevant  
486 correlations between the behaviour of the chemical components and natural radionuclides  
487 in the water and the hydrochemistry of the host rock (Table 5). The concentrations below  
488 the detection limit (DL) were replaced with  $\text{DL}/2$  for the statistical analysis, since the  
489 percentage of non-detects was below 15% (U.S. EPA, 2006). From the correlation matrix,  
490 it is possible to observe relevant hydrochemical relationships between the dissolution of  
491 the host rock and the behaviour of the elements and radionuclides in the studied water, as  
492 has been commented throughout this work.

493 **Table 5.** Spearman correlation matrix (non-Gaussian variables). \* Significant  
494 correlations at significant level  $p < 0.05$ .

495

496 The 4 principal factors explain 79% of the sampling variance, although only the first two  
497 are of interest (F1: 38%; F2: 22%). This percentage is relatively low, probably due to the  
498 heterogeneity of the aquifer systems. F1 explains 38% of the total variance and is  
499 determined by pH, EC, DR and the concentration of Ca, Mg,  $\text{HCO}_3^-$  and  $\text{SO}_4^-$  (Figure  
500 7A). The concentration of Ca, Mg and  $\text{HCO}_3^-$  presented a high correlation with EC  
501 (Figure S1, Supplementary Information). Thus, F1 is strongly related to the bulk  
502 dissolution factor of the host rock. In the observation plot (Figure 7B), two groups of  
503 waters can be distinguished: one is characterised by water from highly carbonated  
504 aquifers (NAT, SOL, CAZ, AQB, VEL, REG and SIS) and the other one is characterised  
505 by granitic host rock (AQA, SIF, AGS, MON, CAB, LAN and VIR). On the other hand,  
506 F2 explains 22% of the total variance and is determined mainly by Cl concentration, gross  
507 alpha,  $^{226}\text{Ra}$  and  $^{228}\text{Ra}$  activity concentration, probably associated with the presence of  
508 chloride salts in solution.

509 **Figure 7.** PCA results plot of variables (a) and observations (b).

510 With respect to the physicochemical parameters,  $^{238}\text{U}$  presents a relatively positive  
511 correlation with Sr (0.66) and As (0.60), whereas  $^{234}\text{U}$  shows correlation with Sr (0.76),  
512 Ca (0.65),  $\text{SO}_4^-$  (0.64), pH (0.62),  $\text{HCO}_3^-$  (0.58), DR (0.57) and EC (0.56). This is the  
513 reason why  $^{234}\text{U}/^{238}\text{U}$  has the same positive correlations (pH, EC, DR, Ca, Mg and  $\text{HCO}_3^-$   
514 ). These relationships are associated with the dissolution of the carbonated host rock.

515 Moreover, the gross alpha presents a positive correlation with  $^{238}\text{U}$  (0.67),  $^{226}\text{Ra}$  (0.67)  
516 and  $^{234}\text{U}$  (0.55), as was expected, since they are emitters of alpha particles. Likewise,  
517  $^{226}\text{Ra}$  shows a positive correlation with  $^{228}\text{Ra}$  (0.83), probably due to their similar  
518 chemical behaviour, Cl (0.56), possibly due to the existence of soluble complexes, and  
519  $^{238}\text{U}$  (0.54), which is its decay series parent.

520 On the contrary,  $^{210}\text{Pb}$  has a negative correlation with  $^{234}\text{U}/^{238}\text{U}$  (-0.80), Ca (-0.71), pH (-  
521 0.61),  $\text{HCO}_3^-$  (-0.60), EC (-0.57) and DR (-0.57), whereas it only presents a positive  
522 correlation with Cs (0.71) and  $^{226}\text{Ra}/^{234}\text{U}$  (0.70).

### 523 **3.5. INDICATIVE DOSE**

524 The Concentration Index (CI) of the analysed waters from Equation 1 is shown in Table  
525 6. Most of the waters presented a very low CI; specifically, 80 % showed a CI in a range  
526 of 0.02-0.35. On the other hand, AQA and MON had a  $\text{CI} > 0.5$ . SIF is the only water  
527 that obtained a CI above 1, suggesting that it could exceed the parametric value of 0.1  
528 mSv. The high values are mainly due to the activity concentration of  $^{226}\text{Ra}$ ,  $^{228}\text{Ra}$ ,  $^{210}\text{Pb}$   
529 and  $^{210}\text{Po}$  present in these waters, which in turn are related to the granitic host rock.

530 The CI parameter only indicates whether some waters could exceed the parametric value  
531 (0.1 mSv/year); for more accurate information, the dose received by ingestion should be  
532 calculated. Table 5 shows the estimated annual doses by internal exposure from drinking  
533 SIF, AQA and MON waters ( $\text{CI} > 0.5$ ). The results indicate that only SIF waters among  
534 the investigated aquifers exceed the parametric value (0.1 mSv).

535 **Table 6.** *Estimated annual indicative doses (ID) (mSv) by ingestion of 730 L year<sup>-1</sup> for*  
536 *adults from some bottled mineral waters.*

### 537 **4. CONCLUSION**

538 In this work, fifteen different brands of bottled drinking water from different regions of  
539 Spain were characterised physicochemically and radiologically. The aims were to  
540 evaluate their quality according to the current Spanish legislation of water intended for  
541 human consumption, as well as to analyse the behaviour of the natural radionuclides  
542 according to the hydrogeology of the water springs.

543 The waters presented a neutral character (pH around 6-7) and a low mineralization (DR  
544  $< 500 \text{ mg L}^{-1}$ ), with carbonate and calcium being the major ions present in aquifers with  
545 carbonated lithology, whereas Si, Na and Cl were the main elements found in granitic  
546 aquifers. From the physicochemical point of view, the waters complied with the criteria  
547 of Spanish regulations.

548 The bottled mineral waters presented a high variability in concentrations of natural  
549 radionuclides, which depend on the geology and hydrochemical conditions of the aquifer.  
550 Several waters exceeded the parametric value for gross alpha, mainly due to  $^{234}\text{U}$ ,  $^{226}\text{Ra}$   
551 and/or  $^{210}\text{Pb}$  concentrations. These natural radionuclides are easily leached from the host  
552 rock into the water under certain conditions.  $^{234}\text{U}$  is easily leachate in presence of high  
553 concentration of carbonate in solutions.  $^{226}\text{Ra}$  in water is mainly related to the existence  
554 of high concentration of chloride ions and  $^{210}\text{Pb}$  with the reduction conditions of aquifers.  
555 The estimated annual indicative doses calculated by ingestion indicated that SIF exceed  
556  $0.1 \text{ mSv}$  per year. The natural radionuclides that contribute to the indicative doses are  
557 especially  $^{226}\text{Ra}$  and  $^{210}\text{Pb}$ . In view of these facts, further research is suggested to evaluate  
558 the potential risk to human health.

## 559 **ACKNOWLEDGEMENT**

560 This research was partially supported by the Spanish Ministry of Science, Innovation and  
561 Universities, by projects: 1) “Fluxes of radionuclides emitted by the PG piles located in  
562 Huelva; assessment of the dispersion, radiological risks and remediation proposals” (Ref.:  
563 CTM2015-68628-R), and 2) “Equipment for the improvement of the Unity of  
564 Environmental Radioactivity of the University of Huelva” (Ref.: EQC2018-004306-P). "

## 566 **REFERENCES**



567 Altikulac A., Turhan S., Gumus H., 2015. The natural and artificial radionuclides in  
568 drinking water samples and consequent population doses. *Journal of Radiation Research*  
569 *and Applied Sciences* 8, 578-582.

570 Andreo B. and Carrasco F., 1999. Application of geochemistry and radioactivity in the  
571 hydrogeological investigation of carbonate aquifers (Sierras Blanca and Mijas, southern  
572 Spain). *Applied Geochemistry* 14, 283-299.

573 Ansoborlo E., Berard P., Auwer C. D., Leggett R., Menetrier F., Younes A., Montavon  
574 G., Moisy P., 2012. Review of Chemical and Radiotoxicological Properties of Polonium  
575 for Internal Contamination Purposes. *Chemical Research in Toxicology* 25(8):1551-64.

576 Baeza A., Del Rio L. M., Jimenez A., Miro C. and Paniagua J. M., 1995. Factors  
577 Determining the Radioactivity Levels of Waters in the Province of Caceres (Spain). *Appl.*  
578 *Radiat. Isot.* 46, 1053-1059.

579 Bhatti I.A., Hayat M.A., Iqbal M. 2012. Assessment of thorium in the environment (a  
580 review). *Journal- Chemical Society of Pakistan* 34(4):1012-1022

581 Blanco C., Lozano J.C., Tome F.V., 2002. On the use of  $^{225}\text{Ra}$  as yield tracer and  
582  $\text{Ba}(\text{Ra})\text{SO}_4$  microprecipitation in  $^{226}\text{Ra}$  determination by  $\alpha$ -spectrometry. *Appl. Radiat.*  
583 *Isot.* 57, 785-790.

584 Howell R.J., Alpers C. N., Jamieson H. E., Nordstrom D. K., Majzlan J., 2014. The  
585 Environmental Geochemistry of Arsenic -- An Overview --. *Reviews in Mineralogy &*  
586 *Geochemistry*, 79, 1-16.

587 Carvalho F., Fernandes S., Fesenko S., Holm E., Howard B., Martin P., Phaneuf M.,  
588 Porcelli D., Pröhl G., Twining J., 2017. The Environmental Behaviour of Polonium.  
589 IAEA (International Atomic Energy Agency) Technical Reports Series No. 484.

590 Chau N. D., Dulinski M., Jodlowski P., Nowak J., Rozanski K., Sleziaak M. and Wachniew  
591 P., 2011. Natural radioactivity in groundwater – a review. *Isotopes in Environmental and*  
592 *Health Studies*, 47, 415–437.

593 Clausen J. L., Bostick B. and Korte N., 2011. Migration of Lead in Surface Water, Pore  
594 Water, and Groundwater with a Focus on Firing Ranges. *Critical Reviews in*  
595 *Environmental Science and Technology*, 41:15, 1397-1448.

596 Consejo de seguridad Nuclear (CSN), 2000. Proyecto Marna. Informe Técnico INT-04-  
597 02.

598 COUNCIL DIRECTIVE 2013/51/EURATOM of 22 October 2013 laying down  
599 requirements for the protection of the health of the general public with regard to  
600 radioactive substances in water intended for human consumption.

601 Davis, J.C., 2002. *Statistics and Data Analysis in Geology*, third ed. Dover Phoenix  
602 Editions, New York.

603 Deverel S. J., Goldberg S., and Fujii R., 1990. *Agricultural salinity assessment and*  
604 *management*, second edition. Chapter: Chemistry of trace elements in soils and  
605 groundwater. American Society of Civil Engineers.

606 Dueñas C., Fernandez M. C., Liger E. and Carretero J., 1997. Natural Radioactivity  
607 Levels In Bottled Water in Spain. *Wat. Res.* 31, 1919-1924.

608 Eróss A., Csondor K., Izsák B., Vargha M., Horváth Á., Pándics T., 2018. Uranium in  
609 groundwater – The importance of hydraulic regime and groundwater flow system's  
610 understanding. *Journal of Environmental Radioactivity* 195, 90–96.

611 European Federation of Bottled Waters (EFBW). Abril-2019. ("<https://www.efbw.org/>")

612 Flynn W.W., 1968. The determination of low levels of Polonium-210 in environmental  
613 materials. *Anal. Chim. Acta* 43, 221-227.

614 Galán López M, Martín Sánchez A., 2008. Present status of <sup>222</sup>Rn in groundwater in  
615 Extremadura. *Journal of Environmental Radioactivity* 99, 1539-1543.

616 Giménez-Forcada E. and Vega-Alegre M., 2015. Arsenic, barium, strontium and uranium  
617 geochemistry and their utility as tracers to characterize groundwaters from the Espadán–  
618 Calderona Triassic Domain, Spain. *Science of the Total Environment* 512–513, 599–612.

619 Grandia, F., Merino, J., Bruno, J., 2008. Assessment of the Radium-barium Co-  
620 precipitation and its Potential Influence on the Solubility of Ra in the Near-field. *Svensk*  
621 *Kärnbränslehantering AB, SKB TR-08–07, Stockholm, Sweden. 52 pp.*

622 Grundl, T., Cape, M., 2006. Geochemical factors controlling radium activity in a sand-  
623 stone aquifer. *Ground Water* 44, 518–527.

624 Grupo de Hidrología Subterránea (GHS), Abril 2019.  
625 ([https://h2ogeo.upc.edu/es/software-hidrologia-subterranea/11-software-hidrologia-](https://h2ogeo.upc.edu/es/software-hidrologia-subterranea/11-software-hidrologia-subterranea/42-easy-quim%22)  
626 [subterranea/42-easy-quim%22](https://h2ogeo.upc.edu/es/software-hidrologia-subterranea/42-easy-quim%22))

627 Guerrero J. L., Vallejos A., Ceron J. C., Sanchez-Martos F., Pulido-Bosch A., J. P.  
628 Bolívar, 2016. U-isotopes and <sup>226</sup>Ra as tracers of hydrogeochemical processes in

629 carbonated karst aquifers from arid áreas. *Journal of Environmental Radioactivity* 158-  
630 159, 9-20.

631 Hallstadius L., 1984. A method for the electrodeposition of actinides. *NIM Phys. Res.* 223  
632 (2-3), 266-267.

633 Herranz M., Abelairas A. and Legarda F., 1997. Uranium Contents and Associated  
634 Effective Doses in Drinking Water from Biscay (Spain). *Appl. Radiat. Isot.* Vol. 48, No.  
635 6, pp. 857-861.

636 Holm E., Fukai R., 1977. Method for multi-element alpha-spectrometry of actinides and  
637 its application to environmental radioactivity studies. *Talanta* 24 (11), 659-664.

638 ICRP, 2007. The 2007 Recommendations of the International Commission on  
639 Radiological Protection. ICRP Publication 103. *Ann. ICRP* 37 (2-4).

640 International Atomic Energy Agency (IAEA), 2003. Guidelines for radioelement  
641 mapping using gamma ray spectrometry data, Technical Reports Series No. 1363,  
642 Vienna, Austria.

643 International atomic energy agency (IAEA), 2014. Technical Reports Series No. 476. The  
644 Environmental Behaviour of Radium: Revised Edition.

645 Jankovic M. M., Todorovic D. J., Todorovic N. A., Nikolov J., 2012. Natural  
646 radionuclides in drinking waters in Serbia. *Applied Radiation and Isotopes* 70, 2703–  
647 2710.

648 Jia G., Torri G., Magro L., 2009 Concentrations of  $^{238}\text{U}$ ,  $^{234}\text{U}$ ,  $^{235}\text{U}$ ,  $^{232}\text{Th}$ ,  $^{230}\text{Th}$ ,  
649  $^{228}\text{Th}$ ,  $^{226}\text{Ra}$ ,  $^{228}\text{Ra}$ ,  $^{224}\text{Ra}$ ,  $^{210}\text{Po}$ ,  $^{210}\text{Pb}$  and  $^{212}\text{Pb}$  in drinking water in Italy:

650 reconciling safety standards based on measurements of gross  $\alpha$  and  $\beta$ . Journal of  
651 Environmental Radioactivity 100, 941–949.

652 Jia G. and Torri G., 2007. Estimation of radiation doses to members of the public in Italy  
653 from intakes of some important naturally occurring radionuclides ( $^{238}\text{U}$ ,  $^{234}\text{U}$ ,  $^{235}\text{U}$ ,  
654  $^{226}\text{Ra}$ ,  $^{228}\text{Ra}$ ,  $^{224}\text{Ra}$  and  $^{210}\text{Po}$ ) in drinking water. Applied Radiation and Isotopes 65,  
655 849–857.

656 Jolliffe, I.T., 2002. Principal Component Analysis, second ed. (Springer Series in  
657 Statistics). Smedley P.L., Kinniburgh D.G. A review of the source, behaviour and  
658 distribution of arsenic in natural waters. Applied Geochemistry 17 (2002) 517–568.

659 Karamanis D., Stamoulis K., Ioannides K.G., 2007. Natural radionuclides and heavy  
660 metals in bottled water in Greece. Desalination 213, 90–97.

661 Khandaker M. U., Mohd Nasir N. L., Zakirin N. S., Kassim H. A., Asaduzzaman K.,  
662 Bradley D.A, Zulkifli M.Y., Hayyan. A., 2017. Radiation dose to the Malaysian populace  
663 via the consumption of bottled mineral water. Radiation Physics and Chemistry 140, 173–  
664 179.

665 Korkmaz Görür F., Keser R., Dizman S., Okumuşoğlu N.T., 2011. Annual effective dose  
666 and concentration levels of gross  $\alpha$  and  $\beta$  in various waters from Samsun, Turkey.  
667 Desalination 279, 135–139.

668 Kozłowska B., Walencik A., Dorda J., Przylibski T.A., 2007. Uranium, radium and  
669  $^{40}\text{K}$  isotopes in bottled mineral waters from Outer Carpathians, Poland. Radiation  
670 Measurements 42, 1380 – 1386.

671 Kralik C., Friedrich M., Vojir F., 2003. Natural radionuclides in bottled water in Austria.  
672 Journal of Environmental Radioactivity 65, 233–241.

673 Man Y. and Hooda P. S., 2010. Trace elements in soil. Chapter: Chromium, Nickel and  
674 Cobalt. Wiley.

675 Manjon G., Vioque I., Moreno H., Garcia-Tenorio R. and García-Leon M., 1997.  
676 Determination of  $^{226}\text{Ra}$  and  $^{224}\text{Ra}$  in Drinking Waters by Liquid Scintillation Counting.  
677 Appl. Radiat. Isot. 48, 535-540.

678 Manu A., Santhanakrishnan V., Rajaram S., P.M Ravi., 2014. Concentration of natural  
679 radionuclides in raw water and packaged drinking water and the effect of water treatment.  
680 Journal of Environmental Radioactivity 138, 456-459.

681 Markich S. J., 2002. Uranium Speciation and Bioavailability in Aquatic Systems: An  
682 Overview. The Scientific World Journal 2, 707-729.

683 Martin Sanchez A., Rubio Montero M.P., Gomez Escobar V., Jurado Vargas M., 1999.  
684 Radioactivity in bottled mineral waters. Applied Radiation and Isotopes 50, 1049-1055.

685 Ortega X., Vaks I., and Serrano I., 1996. Natural Radioactivity in Drinking Water in  
686 Catalonia (Spain). Environment International, 22, S347-S354.

687 Palomo M., Peñalver A., Borrull F., Aguilar C., 2007. Measurement of radioactivity in  
688 bottled drinking water in Spain. Applied Radiation and Isotopes 65, 1165–1172.

689 Pérez-Moreno S.M., Gázquez M.J., Casas-Ruiz M., San Miguel E.G., Bolívar J.P., 2019.  
690 An improved method for radium-isotopes quartet determination by alpha particle  
691 spectrometry by using  $^{225}\text{Ra}$  ( $^{229}\text{Th}$ ) as isotopic tracer. Journal of Environmental  
692 Radioactivity 196, 113–124.

693 Piper, A. M., 1953. A graphic procedure I the geo-chemical interpretation of water  
694 analysis, USGS Groundwater Note no, 12.

695 Porcelli D., 2014. A method for determining the extent of bulk  $^{210}\text{Po}$  and  $^{210}\text{Pb}$   
696 adsorption and retardation in aquifers. *Chemical Geology* 382, 132–139

697 RD 1798/2010. Real Decreto 1798/2010, de 30 de diciembre, por el que se regula la  
698 explotación y comercialización de aguas minerales naturales y aguas de manantial  
699 envasadas para consumo humano. *Boletín Oficial del Estado*, 19 de enero de 2011, núm.  
700 6, pp. 6111 a 6133

701 RD 314/2016. Real Decreto 314/2016, de 29 de julio, por el que se modifican el Real  
702 Decreto 140/2003, de 7 de febrero, por el que se establecen los criterios sanitarios de la  
703 calidad del agua de consumo humano, el Real Decreto 1798/2010, de 30 de diciembre,  
704 por el que se regula la explotación y comercialización de aguas minerales naturales y  
705 aguas de manantial envasadas para consumo humano, y el Real Decreto 1799/2010, de  
706 30 de diciembre, por el que se regula el proceso de elaboración y comercialización de  
707 aguas preparadas envasadas para el consumo humano. *Boletín Oficial del Estado*, 30 de  
708 julio de 2016, núm. 183, pp. 53106 a 53126.

709 RD 783/2001. Real Decreto 783/2001, de 6 de julio, por el que se aprueba el Reglamento  
710 sobre protección sanitaria contra radiaciones ionizantes. *Boletín Oficial del Estado*, 26 de  
711 julio de 2001, núm. 178 pp. 27284 a 27393

712 Rožmarić M., Rogić M., Benedik L., Štrok M., 2012. Natural radionuclides in bottled  
713 drinking waters produced in Croatia and their contribution to radiation dose. *Science of*  
714 *the Total Environment* 437, 53–60.

715 Santschi, P.H., Murray, J.W., Baskaran, M., Benitez-Nelson, C.R., Guo, L.D., Hung, C.-  
716 C., Lamborg, C., Moran, S.B., Passow, U., Roy-Barman, M., 2006. Thorium speciation  
717 in seawater. *Mar. Chem.* 100, 250-268.

718 Shabana E.I. and Kinsara A.A., 2014. Radioactivity in the groundwater of a high  
719 background radiation area. *Journal of Environmental Radioactivity* 137, 181-189.

720 Sherif M. I., Lin J., Poghosyan A., Abouelmagd A., Sultan M. I., Sturchio N. C., 2018.  
721 Geological and hydrogeochemical controls on radium isotopes in groundwater of the  
722 Sinai Peninsula, Egypt. *Science of the Total Environment* 613–614, 877–885.

723 Sherif M.I. and Sturchio N. C., 2018. Radionuclide geochemistry of groundwater in the  
724 Eastern Desert. Egypt. *Applied Geochemistry* 93, 69-80.

725 Sherif, M.I., Sultan, M.I., Sturchio, N.C., 2019. Chlorine isotopes as tracers of solute  
726 origin and age of fossil groundwater from the Eastern Desert of Egypt. *Earth and Plane-  
727 tary Science Letters*, vol. 510, 37-44.

728 Somlai J., Horvath G., Kanyar B., Kovacs T., Bodrogi E., Kavasi N., 2002. Concentration  
729 of  $^{226}\text{Ra}$  in Hungarian bottled mineral water. *Journal of Environmental Radioactivity* 62,  
730 235–240.

731 Stackelberg P. E., Szabo Z., Jurgens B. C., 2018. Radium mobility and the age of  
732 groundwater in public-drinking-water supplies from the Cambrian-Ordovician aquifer  
733 system, north-central USA. *Applied Geochemistry* 89, 34–48.

734 Sturchio, N.C., Banner, J.L., Binz, C.M., Heraty, L.B., Musgrove, M., 2001. Radium  
735 geochemistry of ground waters in Paleozoic carbonate aquifers, midcontinent, USA.  
736 *Appl. Geochem.* 16, 109–122.



737 Szabo, Z., de Paul, V.T., Fischer, J.M., Kraemer, T.F., Jacobsen, E., 2012. Occurrence  
738 and geochemistry of Radium in aquifers used for drinking water in the United States.  
739 *Appl. Geochem.* 27, 729–752.

740 Taboada T., Martínez Cortizas A., García C., García-Rodeja E., 2006. Uranium and  
741 thorium in weathering and pedogenetic profiles developed on granitic rocks from NW  
742 Spain. *Science of the Total Environment* 356, 192– 206.

743 Talvitie N.A., 1972. Electrodeposition of actinides for alpha spectrometric determination.  
744 *Anal. Chem.* 44 (2), 280-283.

745 Tudorache A., Marin C., Ioniță D. E. and Badea I. A., 2018. Assessing Barium and  
746 Strontium Concentrations and Speciation in Groundwater from the Area of the Future  
747 Weak – And – Medium Radioactive Waste Repository Saligny – Romania. *Carpathian*  
748 *Journal of Earth and Environmental Sciences*, 13, 57 – 66.

749 U.S. EPA, 2006. Data Quality Assessment: a Reviewer's Guide (EPA QA/G-9R).  
750 EPA/240/B-06/002.

751 UNE 73340-2:2003. Procedure to obtain samples for the determination of environmental  
752 radioactivity. Analytical methods. Part 2: Rest beta activity index in water by proportional  
753 counter.

754 UNE-EN ISO 10704:2016. Water quality - Measurement of gross alpha and gross beta  
755 activity in non-saline water - Thin source deposit method.

756 United Nations Scientific Committee on the Effects of Atomic Radiation UNSCEAR,  
757 2016. Sources, Effects and Risks of Ionizing Radiation Report.

758 United Nations Scientific Committee on the Effects of Atomic Radiation (UNSCEAR),  
759 2008. Sources and Effects of Ionizing Radiation.

760 Vasile M., Loots H., Jacobs K., Verheyen L., Sneyers L., Verrezen F., Bruggeman M.,  
761 2016. Determination of  $^{210}\text{Pb}$ ,  $^{210}\text{Po}$ ,  $^{226}\text{Ra}$ ,  $^{228}\text{Ra}$  and uranium isotopes in drinking  
762 water in order to comply with the requirements of the EU 'Drinking Water Directive'.  
763 *Applied Radiation and Isotopes* 109, 465–469.

764 Vinson, D.S., Tagma, T., Bouchaou, L., Dwyer, G.S., Warner, N.R., Vengosh, A., 2013.  
765 Occurrence and mobilization of radium in fresh to saline coastal groundwater in-ferred  
766 from geochemical and isotopic tracers (Sr, S, O, H, Ra, Rn). *Appl. Geochem.* 38, 161–  
767 175.

768 Wallner G., Wagner R., Katzlberger C., 2008. Natural radionuclides in Austrian mineral  
769 water and their sequential measurement by fast methods. *Journal of Environmental*  
770 *Radioactivity* 99, 1090-1094.

771 Wu Y., Li J., Wang Y., Xie X., 2018. Variations of uranium concentrations in a multi-  
772 aquifer system under the impact of surface water-groundwater interaction. *Journal of*  
773 *Contaminant Hydrology* 211, 65–76.

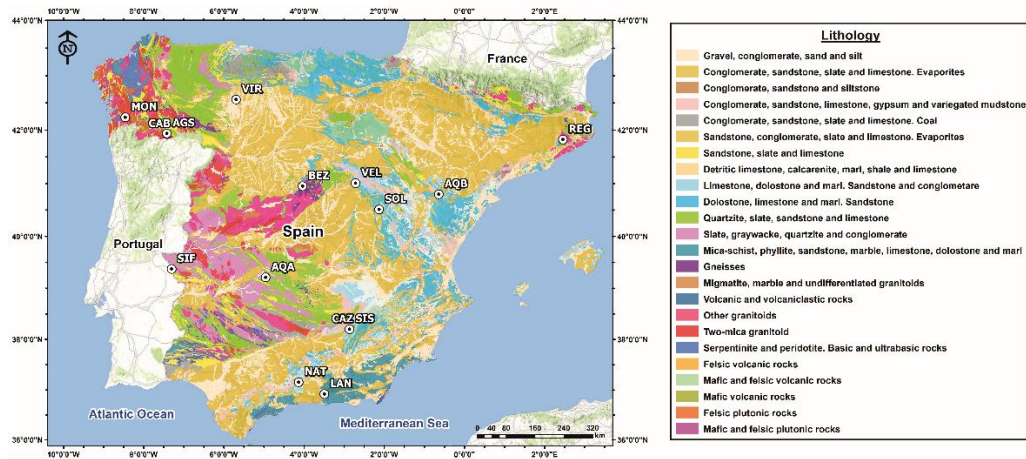


**Figure 1.** General lithological map of Spain and the location of the bottled water sources analysed.

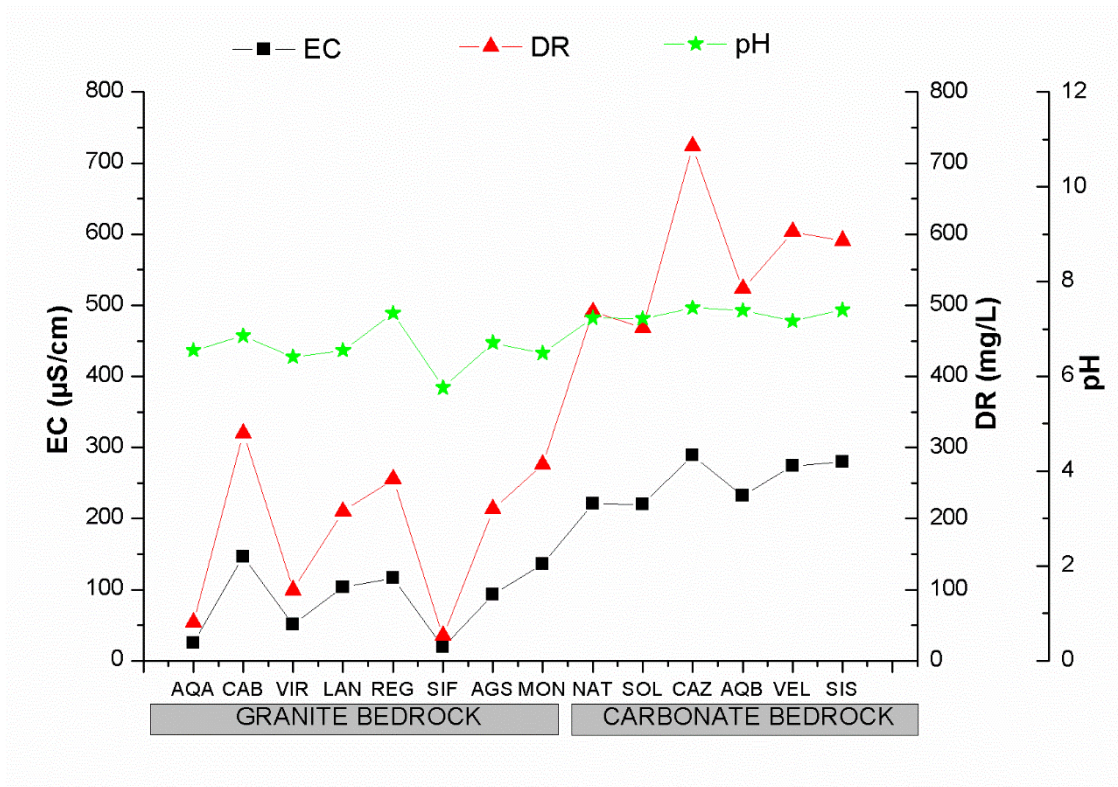


**Figure 2.** pH, EC and DR values of the bottled waters analysed.

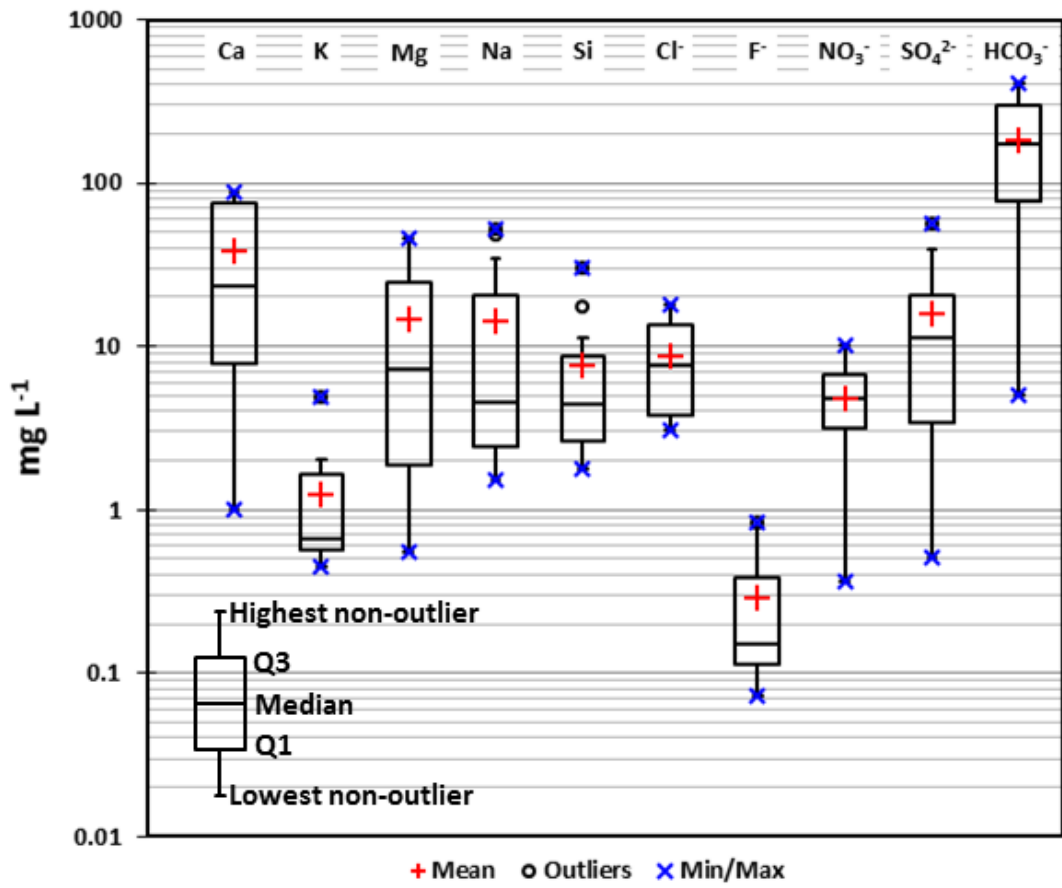
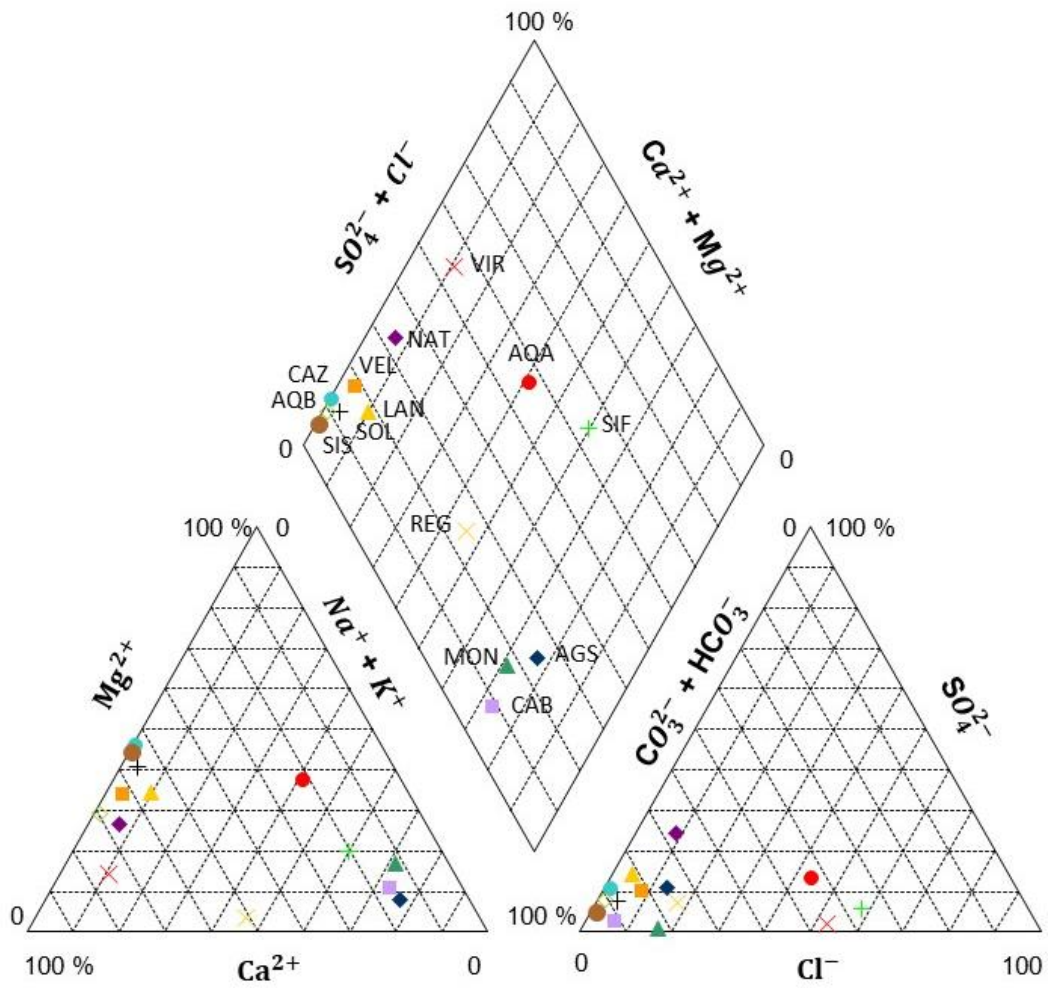
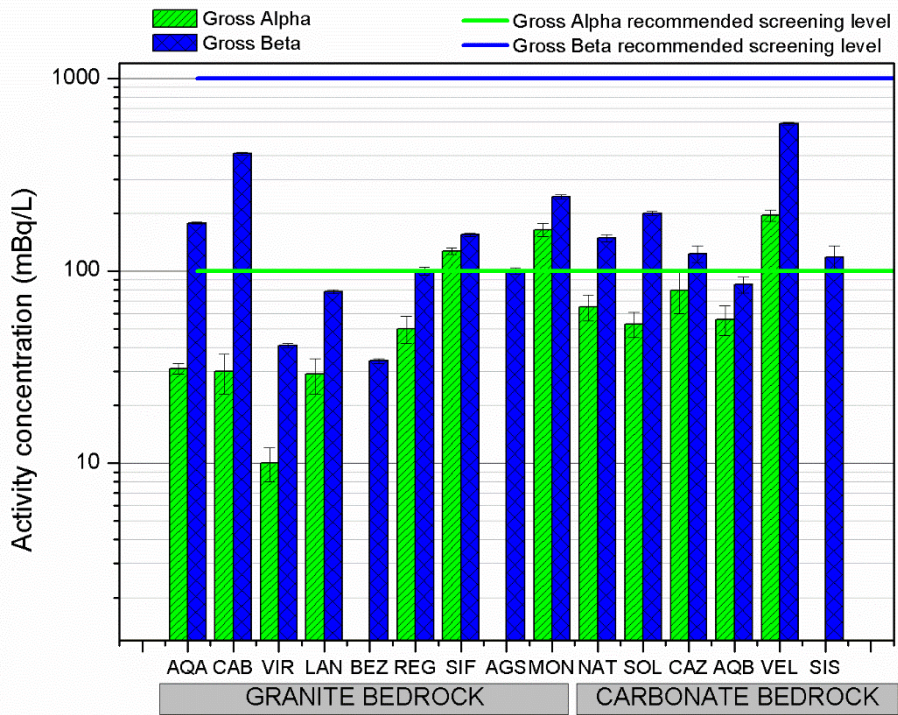


Figure 3. Box and whisker plots of major elements and ions.



● AQA ◆ NAT ■ CAB × VIR + SOL ● CAZ ◇ AQB ▲ LAN ■ VEL × REG + SIF ● SIS ◆ AGS ▲

**Figure 4.** Piper diagram of the bottled water sources.



**Figure 5.** Gross  $\alpha$  and  $\beta$  activity concentrations of the analysed water samples ( $DL=10 \text{ mBq L}^{-1}$ ).

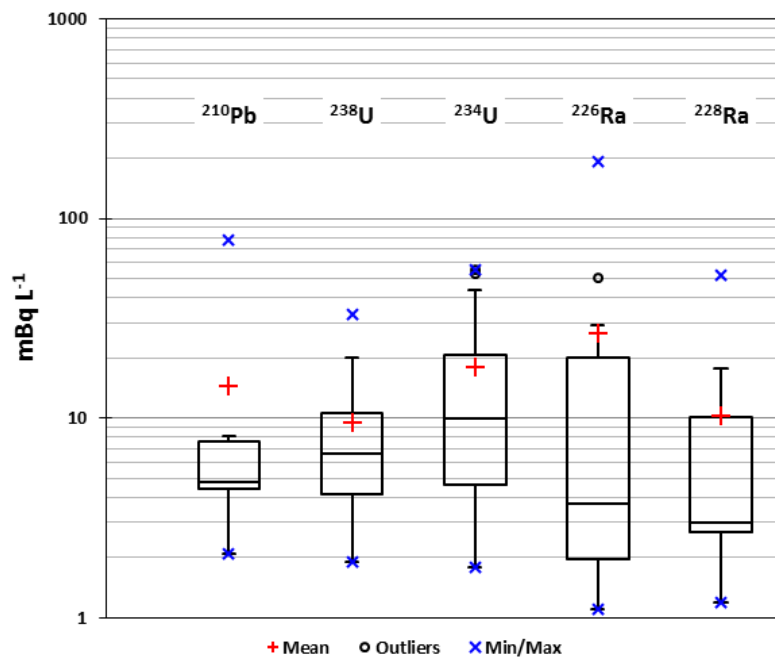


**Figure 6.** Box and whisker plots of natural radionuclide activity concentrations.

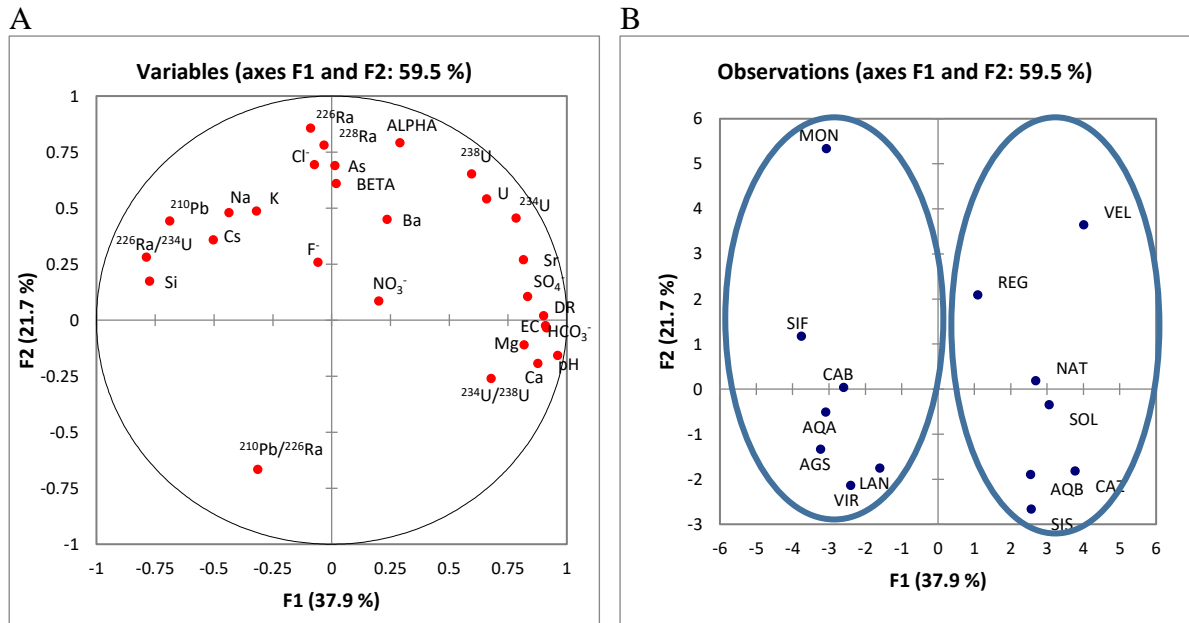


**Figure 7.** PCA results plot of variables (a) and observations (b).

Code	Commercial Name	Batch	Province (Region)	Rock
1A-AQA	Aquarel	L616679412	Badajoz (Extremadura)	Igneous and metamorphic (granites and gneisses)
1B-AQA	Aquarel	L618379412		
1C-AQA	Aquarel	L616779412		
2A-NAT	Font Natura	8429359275006	Granada (Andalucía).	Carbonated (limestones)
2B-NAT	Font Natura	8480017269966		
2C-NAT	Font Natura	8429359275006		
3A-CAB	Cabreiroá	L:14-09-17 18:29	Orense (Galicia)	Igneous (granites)
3B-CAB	Cabreiroá	L:27-12-17 11:27		
4-VIR	Virgen del Camino	170GDMML 08:55	León (Castilla y León).	Sedimentary (Conglomerates and siliceous gravels)
5A-SOL	Solán de Cabras	L0261691256	Cuenca (Castilla La Mancha).	Carbonated (limestones)
5B-SOL	Solán de Cabras	L0261820852		
6-CAZ	Cazorla	L-27/01/18-1	Jaén (Andalucía).	Carbonated (limestones and dolomites)
7A-AQB	Aquabona	C2X1844	Teruel (Aragón).	Carbonated (limestones and dolomites)
7B-AQB	Aquabona	02M2048		
8A-LAN	Lanjarón	L-29-06-18 E21:45	Granada (Andalucía).	Metamorphic (schists)
8B-LAN	Lanjarón	L-04-07-18 E08:38		
8C-LAN	Lanjarón	L-02-06-18 E19:38		
9A-BEZ	Bezoya	LC1596	Segovia (Castilla y León).	Metamorphic (gneisses)
9B-BEZ	Bezoya	LE1746		
10A-VEL	Font Vella	L:10-06-18 JJ10:18	Guadalajara (Castilla La Mancha).	Carbonated (limestones and dolomites)
10B-VEL	Font Vella	L:22-06-18 J21:57		
10C-VEL	Font Vella	L:09-06-18 K20:52		
11-REG	Font de Regás	1411 L16167	Girona (Cataluña).	Granites and gneisses
12-SIF	Sierra Fría	27F0401	Cáceres (Extremadura)	Granites and gneisses
13-SIS	Sierra de Segura	L-17/06/18-6	Jaén (Andalucía).	Carbonated (limestones and dolomites)
14-AGS	Aguas de Sousas	07/07/2016 8:50	Ourense (Galicia).	Granites and gneisses
15-MON	Mondariz	020818-1121	Pontevedra (Galicia).	Granites and gneisses

**Table 1.** Summarised information of the different brands of bottled water analysed.



Samples	Certified activity values (Bq/kg)	Measured activity values (Bq/kg)	$Z_{\text{score}} = \frac{ X_{\text{measured}} - X_{\text{certified}} }{\sqrt{\sigma_{\text{measured}}^2 - \sigma_{\text{certified}}^2}}$
Gross alpha			
CSN-2016	282 ± 56	279 ± 32	0.05
CSN-2017	0.113 ± 0.004	0.184 ± 0.006	0.07
CSN-2018	36 ± 21	51 ± 12	0.65
Gross beta			
CSN-2016	570 ± 114	640 ± 18	0.61
CSN-2017	1.39 ± 0.03	1.66 ± 0.03	0.27
CSN-2018	625 ± 52	686 ± 14	1.15

**Table 2.** Gross alpha and beta activity concentrations obtained in the intercomparison exercises organised by the Spanish Nuclear Safety Commission (CSN).

Samples	Radionuclides	Certified activity values (Bq/kg)	Measured activity values (Bq/kg)	Zscore
CSN-2008	<sup>210</sup> Po	568 ± 157	574 ± 28	0.04
	<sup>238</sup> U	55 ± 10	55 ± 4	0.03
	<sup>234</sup> U	56 ± 10	55 ± 4	0.07
	<sup>230</sup> Th	332 ± 66	335 ± 11	0.05
	<sup>232</sup> Th	6.1 ± 1.2	6.5 ± 0.8	0.28
	<sup>226</sup> Ra	573 ± 115	607 ± 25	0.54
IAEA-326	<sup>210</sup> Po	25.7 ± 9.0	31.3 ± 1.9	0.62
	<sup>238</sup> U	29.4 ± 2.8	23.5 ± 1.6	1.53
	<sup>234</sup> U	29.3 ± 2.8	24.5 ± 1.6	1.81
	<sup>230</sup> Th	34.1 ± 4.6	33.3 ± 2.5	0.15
	<sup>232</sup> Th	39.4 ± 3.6	39.8 ± 2.7	0.09
	<sup>226</sup> Ra	32.6 ± 3.2	35.7 ± 3.0	1.00
	<sup>228</sup> Ra	40.1 ± 0.6	38.8 ± 9.2	0.40
IAEA-327	<sup>210</sup> Po	28.4 ± 9.8	33.7 ± 2.1	0.53
	<sup>238</sup> U	32.8 ± 2.0	29.1 ± 2.5	1.8
	<sup>234</sup> U	31.9 ± 3.0	27.1 ± 2.4	0.71
	<sup>230</sup> Th	34.1 ± 3.4	31.7 ± 1.9	0.62
	<sup>232</sup> Th	38.7 ± 3.0	40.6 ± 2.2	0.51
	<sup>226</sup> Ra	34.1 ± 2.8	29.7 ± 2.5	1.69
	<sup>228</sup> Ra	38.7 ± 1.8	38.1 ± 8.7	0.07

**Table 3.** Results obtained in the intercomparison exercises and certified reference materials.

Samples	<sup>238</sup> U (mBq/L)	<sup>234</sup> U (mBq/L)	<sup>226</sup> Ra (mBq/L)	<sup>210</sup> Pb (mBq/L)	<sup>228</sup> Ra (mBq/L)	<sup>234</sup> U/ <sup>238</sup> U	<sup>226</sup> Ra/ <sup>234</sup> U	<sup>210</sup> Pb/ <sup>226</sup> Ra	<sup>228</sup> Ra/ <sup>226</sup> Ra	CI
DC*	2800	3000	500	100	200	-	-	-	-	-
AQA-1	1.8 ± 0.2	2.8 ± 0.3	34 ± 3	31 ± 1	37 ± 7	1.6 ± 0.2	12 ± 2	0.91 ± 0.09	1.1 ± 0.2	0.72
AQA-2	1.9 ± 0.2	3.3 ± 0.3	27 ± 3	36 ± 1	26 ± 6	1.7 ± 0.2	8 ± 1	1.3 ± 0.2	1.0 ± 0.2	0.73
AQA-3	2.1 ± 0.2	2.9 ± 0.3	26 ± 3	43 ± 1	39 ± 7	1.4 ± 0.2	9 ± 1	1.7 ± 0.2	1.5 ± 0.3	0.89
CAB-1	<LD	<LD	<LD	4.8 ± 0.7	<LD	-	-	-	-	0.06
CAB-2	<LD	<LD	3.7 ± 0.3	6.0 ± 0.9	1.2 ± 0.5	-	-	1.6 ± 0.3	0.3 ± 0.1	0.07
VIR	<LD	<LD	1.1 ± 0.1	<LD	1.3 ± 0.4	-	-	-	1.2 ± 0.4	0.01
BEZ-1	1.9 ± 0.3	1.8 ± 0.3	2.4 ± 0.2	1.4 ± 0.5	3.4 ± 0.7	0.95 ± 0.22	1.3 ± 0.2	0.58 ± 0.21	1.4 ± 0.3	0.04
BEZ-2	<LD	<LD	<LD	5.0 ± 0.9	2.5 ± 0.6	-	-	-	-	0.09
REG	33 ± 2	53 ± 3	5.7 ± 0.3	2.8 ± 0.5	13 ± 1	1.6 ± 0.1	0.11 ± 0.01	0.49 ± 0.09	2.3 ± 0.2	0.15
SIF	6.9 ± 0.5	6.1 ± 0.4	50 ± 2	78 ± 3	7.3 ± 0.8	0.88 ± 0.09	8.2 ± 0.6	1.6 ± 0.1	0.1 ± 0.1	1.31
AGS	<LD	<LD	2.3 ± 0.2	4.6 ± 0.5	2.5 ± 0.5	-	-	2.0 ± 0.3	1.1 ± 0.2	0.09
MON	5.1 ± 1.1	5.1 ± 1.0	194 ± 9	7.1 ± 0.8	52 ± 4	1.0 ± 0.3	38 ± 8	0.04 ± 0.01	0.3 ± 0.1	0.76
<b>MEAN</b>	<b>7.5 ± 3.3</b>	<b>11 ± 5</b>	<b>35 ± 17</b>	<b>20 ± 7</b>	<b>17 ± 5</b>	<b>1.3 ± 0.1</b>	<b>11 ± 3.7</b>	<b>1.1 ± 0.2</b>	<b>1.0 ± 0.2</b>	<b>0.41 ± 0.13</b>
NAT-1	9.6 ± 0.9	11 ± 1	8.0 ± 0.5	4.8 ± 0.6	2.6 ± 0.8	1.1 ± 0.1	0.73 ± 0.08	0.60 ± 0.09	0.3 ± 0.1	0.11
NAT-2	8.3 ± 0.8	8.9 ± 0.8	6.9 ± 0.4	<LD	2.6 ± 1.1	1.1 ± 0.1	0.78 ± 0.08	-	0.4 ± 0.2	0.03
NAT-3	8.7 ± 0.7	11 ± 1	7.5 ± 0.4	<LD	3.2 ± 0.8	1.3 ± 0.2	0.68 ± 0.07	-	0.4 ± 0.1	0.04
SOL-1	17 ± 1	50 ± 2	9.0 ± 0.7	<LD	5.7 ± 1.3	2.9 ± 0.2	0.18 ± 0.02	-	0.6 ± 0.2	0.07
SOL-2	23 ± 2	60 ± 5	13 ± 1	<LD	5.6 ± 1.4	2.6 ± 0.3	0.22 ± 0.02	-	0.4 ± 0.1	0.08
CAZ	6.3 ± 1.2	12 ± 2	2.2 ± 0.2	2.1 ± 0.7	2.9 ± 0.7	1.9 ± 0.5	0.18 ± 0.03	0.95 ± 0.33	1.3 ± 0.3	0.06
AQB-1	6.2 ± 1.2	14 ± 2	1.2 ± 0.2	<LD	3.0 ± 0.6	2.3 ± 0.5	0.09 ± 0.02	-	2.5 ± 0.7	0.02
AQB-2	8.0 ± 1.7	12 ± 2	1.7 ± 0.2	<LD	2.7 ± 0.6	1.5 ± 0.4	0.14 ± 0.03	-	1.6 ± 0.4	0.02
LAN-1	3.5 ± 1.0	3.6 ± 0.9	1.6 ± 0.2	8.5 ± 0.6	3.4 ± 0.6	1.0 ± 0.4	0.44 ± 0.12	5.3 ± 0.8	2.1 ± 0.5	0.15
LAN-2	2.8 ± 1.3	2.3 ± 0.9	2.0 ± 0.3	7.6 ± 0.6	5.2 ± 0.9	0.96 ± 0.57	0.74 ± 0.30	3.8 ± 0.6	2.6 ± 0.6	0.15
LAN-3	4.0 ± 0.9	3.5 ± 0.8	1.6 ± 0.3	8.1 ± 0.6	8.6 ± 1.4	0.95 ± 0.31	0.42 ± 0.13	5.1 ± 1.0	5.4 ± 1.3	0.17
VEL-1	19 ± 4	52 ± 9	90 ± 3	4.3 ± 0.5	17 ± 1	2.7 ± 0.7	1.7 ± 0.3	0.05 ± 0.01	0.2 ± 0.1	0.35
VEL-2	14 ± 2	39 ± 5	76 ± 3	4.1 ± 0.5	15 ± 1	2.8 ± 0.5	1.9 ± 0.3	0.05 ± 0.01	0.2 ± 0.1	0.31
VEL-3	13 ± 4	40 ± 12	85 ± 3	<LD	21 ± 2	3.1 ± 1.3	2.1 ± 0.6	-	0.3 ± 0.1	0.29
SIS	4.4 ± 1.6	9.7 ± 2.6	1.3 ± 0.2	<LD	2.6 ± 0.6	2.2 ± 1.0	0.13 ± 0.04	-	2.0 ± 0.6	0.02
<b>MEAN</b>	<b>9.9 ± 1.8</b>	<b>22 ± 6</b>	<b>20 ± 9</b>	<b>5.6 ± 0.7</b>	<b>6.7 ± 1.6</b>	<b>1.9 ± 0.2</b>	<b>0.7 ± 0.2</b>	<b>2.3 ± 0.6</b>	<b>1.4 ± 0.4</b>	<b>0.13 ± 0.03</b>

**Table 4.** Activity concentrations ( $\text{mBq L}^{-1}$ ) of  $^{210}\text{Pb}$ ,  $^{238-234}\text{U}$ ,  $^{228-226}\text{Ra}$ , activity ratios of  $^{234}\text{U}/^{238}\text{U}$ ,  $^{226}\text{Ra}/^{234}\text{U}$ ,  $^{210}\text{Pb}/^{226}\text{Ra}$  and  $^{226}\text{Ra}/^{228}\text{Ra}$  ( $\text{DL} = 1 \text{ mBq L}^{-1}$ ) and Concentration Index (CI). \*Derived Concentrations (DC) for radioactivity in water intended for human consumption (RD 314/2016).

Variables	pH	EC	DR	As	Ba	Ca	Cs	K	Mg	Na	Si	Sr	U	Cl <sup>-</sup>	F <sup>-</sup>	NO <sub>3</sub> <sup>-</sup>	SO <sub>4</sub> <sup>-</sup>	HCO <sub>3</sub> <sup>-</sup>	ALPHA	BETA	<sup>238</sup> U	<sup>234</sup> U	<sup>226</sup> Ra	<sup>228</sup> Ra	<sup>210</sup> Pb	<sup>234</sup> U/ <sup>238</sup> U	<sup>226</sup> Ra/ <sup>234</sup> U	<sup>210</sup> Pb/ <sup>226</sup> Ra				
pH	<b>1.00</b>																															
EC	<b>0.84</b>	<b>1.00</b>																														
DR	<b>0.83</b>	<b>0.99</b>	<b>1.00</b>																													
As	-0.28	-0.15	-0.16	<b>1.00</b>																												
Ba	-0.04	0.15	0.13	0.50	<b>1.00</b>																											
Ca	<b>0.86</b>	<b>0.91</b>	<b>0.89</b>	-0.05	0.27	<b>1.00</b>																										
Cs	-0.28	-0.27	-0.25	0.09	-0.11	-0.49	<b>1.00</b>																									
K	-0.47	-0.14	-0.09	0.21	0.25	-0.36	0.51	<b>1.00</b>																								
Mg	<b>0.70</b>	<b>0.90</b>	<b>0.88</b>	-0.13	0.16	<b>0.82</b>	-0.34	-0.12	<b>1.00</b>																							
Na	-0.31	-0.24	-0.20	0.02	0.09	-0.47	<b>0.79</b>	<b>0.76</b>	-0.35	<b>1.00</b>																						
Si	<b>-0.56</b>	<b>-0.67</b>	<b>-0.64</b>	-0.09	-0.05	<b>-0.76</b>	<b>0.72</b>	0.52	<b>-0.70</b>	<b>0.76</b>	<b>1.00</b>																					
Sr	<b>0.75</b>	<b>0.73</b>	<b>0.73</b>	0.20	0.40	<b>0.78</b>	-0.08	-0.10	<b>0.55</b>	-0.04	-0.44	<b>1.00</b>																				
U	0.49	0.41	0.42	0.53	0.33	0.49	-0.26	-0.07	0.29	-0.11	-0.39	<b>0.72</b>	<b>1.00</b>																			
Cl <sup>-</sup>	-0.22	-0.06	0.01	0.18	0.38	-0.18	0.13	0.45	-0.20	<b>0.54</b>	0.20	0.16	0.24	<b>1.00</b>																		
F <sup>-</sup>	0.21	0.17	0.20	-0.14	0.05	-0.02	<b>0.79</b>	0.40	-0.03	<b>0.78</b>	0.52	0.29	-0.04	0.21	<b>1.00</b>																	
NO <sub>3</sub> <sup>-</sup>	0.08	0.32	0.37	0.21	-0.28	0.22	0.14	0.22	0.25	-0.03	-0.29	0.13	0.05	-0.09	0.09	<b>1.00</b>																
SO <sub>4</sub> <sup>-</sup>	<b>0.77</b>	<b>0.78</b>	<b>0.79</b>	0.15	0.17	<b>0.82</b>	-0.14	-0.17	<b>0.77</b>	-0.19	<b>-0.58</b>	<b>0.79</b>	<b>0.58</b>	-0.11	0.18	0.42	<b>1.00</b>															
HCO <sub>3</sub> <sup>-</sup>	<b>0.84</b>	<b>1.00</b>	<b>0.99</b>	-0.17	0.16	<b>0.90</b>	-0.30	-0.13	<b>0.91</b>	-0.26	<b>-0.66</b>	<b>0.71</b>	0.42	-0.07	0.14	0.28	<b>0.77</b>	<b>1.00</b>														
ALPHA	0.00	0.25	0.29	<b>0.64</b>	0.29	0.15	0.07	0.23	0.16	0.01	-0.24	0.39	<b>0.56</b>	0.43	-0.05	0.38	0.28	0.24	<b>1.00</b>													
BETA	-0.07	0.19	0.24	0.10	-0.13	-0.15	0.26	0.48	0.17	0.41	0.06	-0.02	0.18	0.50	0.18	0.23	0.05	0.20	<b>0.56</b>	<b>1.00</b>												
<sup>238</sup> U	0.40	0.37	0.39	<b>0.60</b>	0.36	0.43	-0.20	-0.02	0.24	-0.06	-0.36	<b>0.66</b>	<b>0.97</b>	0.34	-0.02	0.11	0.53	0.38	<b>0.67</b>	0.27	<b>1.00</b>											
<sup>234</sup> U	<b>0.62</b>	<b>0.56</b>	<b>0.57</b>	0.43	0.39	<b>0.65</b>	-0.35	-0.16	0.42	-0.22	-0.48	<b>0.76</b>	<b>0.96</b>	0.17	-0.03	0.03	<b>0.64</b>	<b>0.58</b>	<b>0.55</b>	0.15	<b>0.94</b>	<b>1.00</b>										
<sup>226</sup> Ra	-0.28	-0.16	-0.11	<b>0.58</b>	0.27	-0.29	0.16	0.33	-0.09	0.24	0.07	0.00	0.45	<b>0.56</b>	-0.05	0.02	-0.01	-0.15	<b>0.67</b>	<b>0.57</b>	<b>0.54</b>	0.34	<b>1.00</b>									
<sup>228</sup> Ra	-0.20	-0.15	-0.14	<b>0.65</b>	0.48	-0.18	0.08	0.10	-0.10	0.08	0.08	0.05	0.45	0.35	-0.07	-0.27	-0.04	-0.13	<b>0.62</b>	0.38	0.52	0.44	<b>0.83</b>	<b>1.00</b>								
<sup>210</sup> Pb	<b>-0.61</b>	<b>-0.57</b>	<b>-0.57</b>	0.42	-0.18	<b>-0.71</b>	<b>0.71</b>	0.30	-0.50	0.44	0.52	-0.47	-0.26	0.07	0.24	0.17	-0.34	<b>-0.60</b>	0.22	0.33	-0.15	-0.39	0.45	0.41	<b>1.00</b>							
<sup>234</sup> U/ <sup>238</sup> U	<b>0.59</b>	<b>0.63</b>	<b>0.67</b>	-0.44	-0.04	<b>0.62</b>	<b>-0.62</b>	-0.09	<b>0.61</b>	-0.32	-0.46	0.33	0.29	-0.02	-0.20	0.05	0.42	<b>0.68</b>	-0.02	0.15	0.19	0.42	-0.21	-0.25	<b>-0.80</b>	<b>1.00</b>						
<sup>226</sup> Ra/ <sup>234</sup> U	<b>-0.82</b>	<b>-0.61</b>	<b>-0.57</b>	0.04	-0.18	<b>-0.81</b>	0.43	0.42	-0.51	0.39	0.48	<b>-0.70</b>	<b>-0.57</b>	0.38	-0.02	0.08	<b>-0.65</b>	<b>-0.62</b>	0.14	0.41	-0.44	<b>-0.66</b>	0.41	0.21	<b>0.70</b>	-0.51	<b>1.00</b>					
<sup>210</sup> Pb/ <sup>226</sup> Ra	-0.22	-0.33	-0.37	-0.18	-0.41	-0.22	-0.02	-0.04	-0.12	-0.22	0.15	-0.43	-0.40	<b>-0.77</b>	-0.24	0.10	-0.19	-0.31	<b>-0.59</b>	-0.49	-0.49	-0.46	-0.50	-0.52	0.03	-0.09	-0.08	<b>1.00</b>				

**Table 5.** Spearman correlation matrix (non-Gaussian variables). \* Significant correlations at significant level  $p < 0.05$ .

<b>Samples</b>	<b>ID</b>
<b>SIF</b>	0.12
<b>AQA</b>	0.07
<b>MON</b>	0.08

**Table 6.** *Estimated annual indicative doses (ID) (mSv) by ingestion of 730 L year<sup>-1</sup> for adults from some bottled mineral waters.*